EXPANDING THE CARDIAC CELL SURFACE GLYCOPROTEOME IN THE CONTEXT OF ADVANCED HEARTFAILURE

Dorcas Akinuli, and Rebekah Gundry (University of Nebraska Medical Center(UNMC) Omaha, NE)

Background, Significance, Hypothesis: Cardiomyocyte cell surface glycoproteins play a crucial role in regulating ion channel transport, cell-cell communication, molecular recognition, and signal transduction. In heart failure, the dysregulation of these glycoproteins contributes to cardiomyocyte loss, impaired contractility, and cardiac hypertrophy. Despite their importance, our understanding of how these glycoproteins change in advanced heart failure remains limited. Current methods for cell surface protein capture focus on identifying differentially abundant proteins in cardiomyocytes from failing and non-failing hearts. However, these methods primarily capture N-glycosylated proteins, missing key O-glycosylated and non-glycosylated proteins, which limits our understanding of the full glycoproteome. The current approach involves labelling glycosylated proteins and cleaving off N-glycosylated sugars to generate deamidation peptides, which are used as markers for protein identification in mass spectrometry. While this method provides valuable insights, it overlooks other glycosylation patterns such as O-glycosylation, which are also critical to protein function. To better understand glycoprotein dysregulation in advanced heart failure, a more comprehensive approach is needed—one that captures a broader range of glycoproteins and their glycosylation patterns. We hypothesize that a novel labelling chemistry targeting amino acid residues in cell surface proteins, specifically lysine, will enable the identification of both glycosylated and non-glycosylated proteins. This approach will provide a more comprehensive view of the glycoproteome in advanced heart failure, revealing key insights into glycoprotein dysregulation. We anticipate that this method will not only improve our understanding of glycoprotein function in heart failure but also help identify novel biomarkers and therapeutic targets.

Experimental Design: To test the hypothesis, we utilized the Compiled Interactive Resource for Extracellular and Surface Studies (CIRFESS), an online tool that integrates multiple prediction strategies for annotations relevant for the analysis of cell surface and extracellular proteins by MS and applied it to interrogate the human proteome. CIRFESS identified lysine as an optimal target due to its abundance in cell surface proteins, the availability of labeling chemistries, and the potential to generate tryptic peptides for mass spectrometry identification. A lysine-specific biotinylating reagent, impermeable to the cell membrane, was chosen to ensure specificity for surface proteins. The biotinylating reagent is water-soluble and cleavable, leaving a mass tag that serves as experimental evidence of protein location.

We tested the reagent on B cells and HEK 293T cell lines. Cell viability was assessed using a viability assay to ensure reagent safety. Additionally, a time-course experiment was performed to assess toxicity over time. Labeling efficiency and specificity were evaluated using fluorescence and confocal microscopy, with Hoechst for nuclear staining, WGA-Fluor 488 for membrane staining, and Streptavidin-PE for biotin label detection. Three-dimensional images from these techniques provided detailed views of the labeling patterns.

Data and Results: The labeling reagent was initially tested on B cells for benchmarking and then applied to HEK 293T cells to assess its broad applicability. The reagent did not exhibit toxicity, as no significant changes in cell viability were observed. Fluorescence microscopy revealed that the labeling was confined to the cell surface, with clear perimeter staining of the extracellular membrane. This result demonstrates the effectiveness of this novel labeling approach, which does not rely on the sugars present on the cell surface. This labeling chemistry will be incorporated into the cell capture method for mass spectrometry analysis and subsequently applied to cardiomyocytes.

Conclusion: These results support the hypothesis that targeting amino acid residues for labeling provides a promising and feasible approach for more comprehensive coverage of cardiac cell surface proteins. This method will help identify important proteins, including non-glycosylated ones, and allow for the exploration of glycosylated proteins and their dysregulation patterns in advanced heart failure. Ultimately, this approach may lead to new insights into heart failure mechanisms and the identification of novel biomarkers and therapeutic targets.

RACIAL DISPARITIES IN ARDS RELATED MORTALITIES

Sydney Ball, Nikhil Furtado, Taylor Billings, Abubakar Tauseef (Creighton University School of Medicine, Omaha, NE)

Background: Acute Respiratory Distress Syndrome (ARDS) is a significant cause of morbidity and mortality, especially in critically ill patients, with limited treatment options. This study aimed to analyze long-term trends in ARDS-related mortality in the United States, highlighting demographic and geographic disparities with the hope of identifying specific patterns that can inform targeted interventions to improve ARDS mortality.

Methods: ARDS mortality data was retrieved from the Centers for Disease Control and Prevention Wide-Ranging Online Data for Epidemiologic Research (CDC WONDER) national database to analyze mortality trends between 1999 to 2022**.** Age adjusted mortality rates (AAMRs) were stratified by sex, race, and U.S. census region. Joinpoint regression was used to calculate annual percentage changes (APCs) and average annual percent change (AAPC).

Results: The overall AAMR for ARDS increased from 7.40 (95% CI 7.28 – 7.53) in 1999 to a peak of 21.72 (95% CI 21.54-21.91) in 2021 before declining to 8.49 (95% CI 8.37-8.60) in 2022, with an AAPC of 2.92 (95% CI 0.46- 5.60). American Indians consistently had the highest AAMR, increasing from 13.8 (95% CI 11.12-16.48) in 1999 to 18.89 (95% CI 16.75-21.03) in 2022, with an AAPC of 4.37 (05% CI 1.38-8.15). Conversely, Asians had the lowest AAMR with 7.4 (95% CI 6.55 – 8.25) in 1999, decreasing to 6.17 (95% CI 5.76-6.57) in 2022 with an AAPC of 1.31 (95% CI -1.56-4.53) from 1999-2022.
AAMR trends also varied by gender and race. Across most groups, AAMRs declined between 1999-2017, then sharply increased between 2017-2022, and subsequently decreased between 2022-2022. Regional analyses revealed the highest AAMRs in Black populations in the Northeast and Midwest, with increases between 2017-2020 and declines from 2020-2022.

Conclusion: While ARDS-related mortality declined for most groups from 1999-2017, the Covid-19 pandemic caused sharp increases in mortality in 2020. Disparities persisted among racial groups, particularly American Indian and Black populations, highlighting the need for more equitable healthcare policies. These disparities only highlight the importance of future research into social determinants of health and strategies to minimize ARDS-related mortality, especially as it relates to communities disproportionately affected.

ASSESSING THE PREDICTIVE VALUE OF NON-INVASIVE MEASURES OF CARDIOVASCULAR HEALTH IN PREGNANT WOMEN

Authors: Nicole Bender, Ridhi Chaudhary, Elizabeth Kettler, Sarah Uhm, Cierra Wegner, Audrey Bavari, Cory Karasek, Nathan McWilliams, Anum Akbar, Colman Freel, Rebekah Rapoza, Rebecca Drakowski, Melissa Thoene, Matthew VanOrmer, Corrine Hanson, Teri Mauch, & Ann Anderson-Berry

University of Nebraska Medical Center, Omaha, NE

Background: Pregnancy complications including hypertensive disorders of pregnancy (HDP), pre-term birth, and gestational diabetes have been associated with cardiovascular dysfunction; however, the initial dysfunction likely develops in advance of diagnosis. Vascular reactivity index (VRI) has been used to predict future cardiovascular disease (CVD) risk. We assessed if VRI, as a potential measure of cardiovascular health (CVH) early in pregnancy, is associated with later diagnosis of pregnancy complications. Early detection of cardiovascular dysfunction may allow for earlier treatment promoting improved pregnancy outcomes with fewer complications.

Objective: To assess the predictive value of non-invasive measures of cardiovascular health in identifying pregnant women at risk of developing pregnancy complications.

Methods: This study enrolled 57 pregnant women who completed digital thermal monitoring to calculate a VRI between 24- and 30-weeks of gestation. Maternal diet throughout pregnancy was assessed using the Dietary History Questionnaire III. Information about maternal health was collected from the mother's electronic medical record. A modified version of the American Heart Association's Life's Simple 7 CVH Metrics and the ASCVD Risk Estimator Plus tool (n = 41) were used to assess current maternal CVH and the risk of future CVD development. Descriptive statistics, Kruskal-Wallis, and bivariate logistic regression tests were completed. A p-value of < 0.05 was considered statistically significant.

Results: The median cohort age was 32 years with a median VRI of 1.93. The median modified ASCVD risk was 0.0067. In our cohort, 24 subjects were diagnosed with an HDP, 4 had gestational diabetes, and 4 had pre-term births. VRI was not predictive of HDP ($p = 0.626$, OR = 0.775), preeclampsia ($p = 0.561$, OR = 0.515), pre-term birth ($p = 0.522$, OR = 1.91), or diabetes ($p = 0.522$, OR = 1.861). ASCVD risk and CVH scores were not found to be predictive of any pregnancy complications. VRI was not associated with ASCVD risk ($p = 0.06$) or ideal CVH scores ($p = 0.341$).

Conclusions: These results indicate that VRI, the ASCVD risk calculator, and CVH metrics were not predictive of pregnancy complications in this cohort and may not be sensitive indicators of cardiovascular function in pregnant women. In our study population, most subjects were relatively young, making the assessment of CVH difficult. Future directions include increasing the sample size to better understand data trends with ASCVD risk and VRI, and collecting additional data including medication history, blood lipid levels, and physical activity.

EXPRESSION OF CATHEPSIN G IN MAMMARY TUMOR CELLS AND ITS ROLE IN TUMOR GROWTH AND OSTEOLYTIC BONE METASTASIS

Ridhi Bhola, Reegan Sturgeon, and Rakesh K. Singh
University of Nebraska Medical Center, Omaha, NE

Background: Breast cancer has a high propensity to metastasize to the bone. The resulting lesions are predominantly osteolytic and are associated with patient morbidity and mortality. We have demonstrated that tumor-bone interaction plays an important role in osteolytic bone metastasis mediated by the dysregulation of a unique set of genes. Among these genes, several proteases are up-regulated at the tumor-bone interface, including Cathepsin G, a serine protease. These proteases act as mediators between the tumor and the stroma.

Significance: Previously, we have shown that malignant cells and osteoclasts at the TB interface express higher levels of Cathepsin G, which is critical for osteolytic bone metastasis. The precise role of tumor and host-derived Cathepsin G in osteolytic bone metastasis is unknown.

Hypothesis: In this report, we examined the contribution of tumor-derived Cathepsin G by testing the hypothesis that ectopic expression of Cathepsin G modulates malignant cell phenotype, osteoclast recruitment and activation, and osteolytic metastasis.

Experimental Design: We generated stable mammary tumor cell lines constitutively expressing Cathepsin G (Cl66-CTSG). Cathepsin G-expressing tumor cells showed diminished *in vitro* cell proliferative potential and *in vivo* mammary fat pad tumor growth as compared to vector control transfected Cl66-CMV cells.

Results: We demonstrated that Cathepsin G-overexpressing tumor cells induced osteoclast activation and differentiation *in vitro* and tumor-induced osteolysis *in vivo*. To observe the morphological changes in tumor cells by CTSG, we performed phalloidin staining and live cell imaging using CTSG-treated tumor cells. We observed that CTSG induced the formation of homotypic aggregations of tumor cells. We found that increasing the concentration of CTSG decreases tumor cell proliferation and increases cell cycle arrest.

Conclusion: Our data suggest that tumor-derived Cathepsin G might have distinct tumor-modulating activities in the bone microenvironment by regulating cell proliferation and osteoclast recruitment and activation.

ANALYSIS OF LYMPHOCYTIC LEUEKEMIA TRENDS AMONG GENDER, RACE, AGE, AND REGIONAL GROUPS IN THE BETWEEN 1999-2022: A CDC-WONDER DATABASE STUDY

Shannon Blee, Bob Weng, Taylor Billion, Abubakar Tauseef (Creighton University School of Medicine, Omaha, NE)

Background, Significance, Hypothesis: The prevalence and mortality rates of lymphocytic leukemia (LL) has continued to change over time. While there have been improvements in the treatment of both chronic and acute lymphoid leukemia, the effects of confounding variables, such as sex, age, and regional differences, on mortality rates is poorly understood. Therefore, the purpose of this study is to utilize the Center for Disease Control and Prevention (CDC)-WONDER database to further elucidate age-adjusted mortality rates (AAMRs) for LL in respect to sex, race, age, and regional variations in the U.S. between 1999 to 2022.

Experimental Design: Mortality data for LL was obtained from the CDC WONDER database from 1999-2022. The age-adjusted morality rates (AAMRs) were analyzed, and trends were examined by gender, race, region, state, urban vs. rural, and age. A Jointpoint Regression Program was used to estimate the average annual percentage change for each of these groups.

Data and Results: Between 1999-2022, there was a significant overall decrease in morality from 1999-2018 (APC, -1.49*, 95% CI -1.73 to -1.28), and a significant increase from 2018-2022 (APC, 4.81*, 95% CI 2.89 to 7.84). Men had consistently higher AAMRs, when compared with females, yet females saw more of a decrease in mortality rate (AAPC -0.53* [95% CI -0.79 to -0.26] in females vs. -0.44* [95% CI -0.66 to -0.25] in males). The 85+ years old category had the highest overall crude mortality rate of 48.53 (95% CI 46.41-50.65) in 1999 to 50.45 (95% CI 48.73-52.16) in 2019, after which it experienced a substantial jump in crude mortality to its peak of 62.5 (95% CI 60.5-64.51) in 2021 before starting to decline to 60.47 (95% CI 58.58-62.36) in 2022. For race, the Caucasian/White demographic had the highest AAMR over the years, with 3.58 (95% CI 3.50-3.67) in 1999 to 3.28 (95% CI 3.21-3.34) in 2022, but the American Indian/ Alaska native population saw the largest increase in mortality from 2016-2022 (APC, 11.81*, 95% CI 6.99 to -24.64). The Midwest and the West had consistently higher AAMRs compared to the Northeast and Southern regions, with the Midwest having the highest AAMR and smallest decline in mortality (AAPC in Midwest -0.33* [95% CI = -0.64 to -0.05] vs. in West -0.34* [95% CI = -0.64 to -0.05] vs. Northeast -0.57* [95% CI = -1.07 to -0.21] vs. West -0.34* [95% CI = -0.64 to -0.05]) throughout the time periods. From 1999-2019, Iowa had the largest increase in AAMR (0.24), and from 2019-2022, Kansas had the largest increase in AAMR at 1.47. The rural population had an AAMR of 3.64 (95% CI 3.47 to 3.81) in 1999, which decreased to 3.3 (95% CI 3.15 to 3.44) in 2020 and the urban AAMR was 3.34 in 1999 (95% CI 3.27 to 3.42), and decreased to 2.8 in 2020 (95% CI 2.74 to 3.86)

Conclusion: There has been an overall decrease in LL mortality from 1999-2022; however, the results showed that the mortality varied significantly amongst demographic groups. Many groups experienced an increase in mortality in more recent years, which may have been due to lack of access to care during the COVID-19 pandemic. The Midwest and rural populations saw higher AAMRs, possibly stemming from increased travel distance for treatment. Interestingly, although the non-Hispanic white population had the highest AAMRs, it was the American Indian/ Alaska native population that saw the largest mortality increase from 2016-2022. Given our findings of geographic and socioeconomic biases, healthcare officials and providers will be better equipped to establish and optimize policies and management plans to address existing disparities for LL patients.

USING A NEW GENETICALLY MODIFIED MOUSE MODEL TO STUDY THE ROLE OF THE EXOCYTOTIC CA^{2+} SENSOR DOC2B IN SYNAPTIC TRANSMISSION FROM RETINAL ROD PHOTORECEPTOR CELLS

Kwadwo O. Boateng, C. B. Gurumurthy, Wallace B. Thoreson (UNMC Omaha, NE)

Background, Significance, Hypothesis: One of the first steps in vision involves the transmission of photoreceptor cell light responses to second order neurons. The release of neurotransmitter at rod and cone synapses is regulated by exocytotic Ca^{2+} sensors. At other synapses, the Ca^{2+} sensor Doc2B is thought to control spontaneous release of neurotransmitter. Rod and cone photoreceptor cells exhibit high Doc2B transcript levels. We therefore hypothesized that Doc2B may also control spontaneous vesicle release from rods and that eliminating this sensor would impair transmission of light-evoked signals to downstream neurons.

Experimental Design: To eliminate Doc2B, genetically modified mice were created by the UNMC Genome Engineering core by inserting LoxP sites to flank exon 2 of Doc2B. For selective elimination of Doc2B from rod photoreceptor cells, these mice were crossed with Rho-iCre mice that only express cre-recombinase in rods (Rho-iCre/Doc2B^{flfl}). We examined the distribution and location of Doc2B throughout the retina using immunohistochemistry and mRNA in-situ hybridization (RNAscope). We explored effects on light responses of rods, cones and second-order bipolar cells by using electroretinograms (ERGs). Using whole cell patch clamp recordings, glutamate release was assessed by recording anion currents activated during glutamate uptake in individual rods.

Data and Results: RNAscope analysis and immunohistochemical analysis both showed that Doc2B is predominantly localized in photoreceptor cells, with little expression elsewhere in the retina. Doc2B immunofluorescence was reduced in Rho-iCre/Doc2B^{flfl} mice while cone labeling was unaffected, consistent with elimination of Doc2B from rods but not cones. RNAscope labeling for the Doc2A isoform is absent from wild-type photoreceptors and was not up-regulated in Rho-iCre/Doc2B^{flfl} mice. ERG recordings showed no significant change in the amplitude or kinetics of A-waves (that reflect photoreceptor responses) and B-waves (that reflect second-order bipolar cell responses) suggesting that synaptic transmission from photoreceptors is unimpaired. Spontaneous release of synaptic vesicles measured from glutamate transporter anion currents in rods was not eliminated in Rho-iCre/Doc2B^{flfl} mice, but instead showed a greater propensity for simultaneous multivesicular release.

Conclusion: The results suggest that while Doc2B appears to regulate vesicle release by enhancing the likelihood of multivesicular fusion, it is not required for spontaneous synaptic vesicle release in rods. These modest changes in spontaneous release did not produce significant changes in transmission of light responses assessed with ERGs. While the prominent expression of Doc2B in rods and cones suggests an important role for this Ca^{2+} sensor, that role remains unclear.

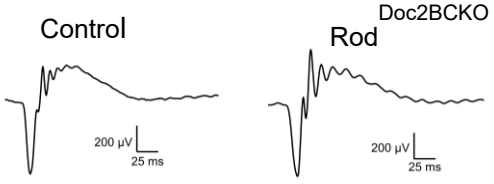

Figure 1. Representative ERG traces of dark-adapted mice

TRENDS IN RECTAL ADENOCARCINOMA INCIDENCE AMONG YOUNGER ADULTS: A TEMPORAL ANALYSIS

John Paul Braun, B.A., Peter T. Silberstein, M.D. (Creighton SOM Omaha, NE)

Background: Rectal adenocarcinoma is a cancer with rising incidence among younger patients. The underlying reasons for this trend remain unclear, particularly concerning the role of socioeconomic and demographic variables. Identifying the contributing factors driving this increase is essential for improving prevention strategies and patient outcomes. This study investigates the relationship between socioeconomic variables and the growing rates of rectal carcinoma in younger populations.

Significance of problem: The rising incidence of rectal adenocarcinoma among younger patients is concerning and points to potential shifts in environmental, genetic, or lifestyle factors. However, the influence of socioeconomic and healthcare access variables on these trends has not been well studied. Investigating these factors is crucial for designing targeted interventions and informing policy changes to address the increasing burden of rectal cancer in young adults.

Hypothesis: The rates of rectal adenocarcinoma are increasing among younger patients, and this increase is compounded by socioeconomic factors, such as race, insurance status, and income level.

Experimental Design: Patients diagnosed with rectal adenocarcinoma between 2004 and 2022 were identified using the NCDB. A total of 440,316 patients were included, with 422,474 patients over 40 years old and 17,842 patients under 40. Logistic regression was used to assess the relationship between demographic and socioeconomic variables (e.g., sex, race, insurance status, Charlson-Deyo comorbidity score, and income level) and the increasing rates of rectal adenocarcinoma in younger patients. Analyses were conducted using SPSS version 29.0.2.0, with statistical significance set at $\alpha = 0.05$.

Results/Data: A total of 440,316 patients were analyzed. Among them, 95.9% were over 40 years old, and 4.1% were younger than 40. The proportion of younger patients increased slightly from 3.6% in 2004 to 4.6% in 2022. Logistic regression revealed that each additional year was associated with a 1.7% increase in the likelihood of being diagnosed with rectal adenocarcinoma as a younger patient (OR = 1.017, $p < 0.001$). Male patients were 24.7% more likely to be younger at diagnosis compared to females (OR = 1.247, $p < 0.001$). Black patients had a 59.3% higher likelihood of being diagnosed at a younger age compared to White patients (OR = 1.593, $p < 0.001$). Low-income status did not significantly affect the odds of younger diagnosis (OR = 1.017, $p = 0.426$). Higher Charlson-Deyo comorbidity scores were associated with lower odds of younger diagnosis (OR = 0.442, $p < 0.001$). Patients with non-private insurance were 41.6% less likely to be diagnosed at a younger age compared to those with private insurance (OR = 0.584, $p < 0.001$). Higher tumor stage was associated with a 3.4% increase in the likelihood of younger diagnosis (OR = 1.034, $p < 0.001$).

Conclusions: This study highlights the increasing rates of rectal adenocarcinoma among younger patients and the significant influence of socioeconomic and demographic factors on the likelihood of younger diagnosis. Notably, lower Charlson-Deyo comorbidity scores were associated with decreased odds of being diagnosed as a younger patient, possibly indicating that healthier individuals are more likely to exhibit the rising trends in rectal carcinoma among youth. Disparities in healthcare access, insurance status, and race also appear to play critical roles in driving these trends. The increase in younger diagnoses over time may reflect shifts in environmental or lifestyle factors, as well as improved diagnostic practices. These results underscore the importance of further research to identify the underlying causes of this rise and to develop targeted strategies to address the unique challenges faced by younger patients with rectal adenocarcinoma. These efforts will be essential in mitigating the rising burden of this disease and improving outcomes for affected individuals.

TITLE: INCREASED MOLAR CONCENTRATIONS OF MALONDIALDEHYDE-ACETALDEHYDE MODIFIED FIBRINOGEN ALTER THE EFECTS OF PDGF AND IL-1BETA SECREATION IN MACROPHAGE.

Cole Bures, Jack E. Mordeson, Wenxian Zhou, Michael J. Duryee, Carlos D. Hunter, Ted R. Mikuls, and Geoffrey M. Thiele (UNMC Omaha, NE)

BACKGROUND, Significance, Hypothesis: Malondialdehyde-acetaldehyde (MAA) adducts are byproducts of lipid peroxidation, which modify positively charged lysine amino acids into neutrally charged MAA adducts. This modification alters the structure of self-proteins, rendering them immunogenic. Elevated levels of anti-MAA antibodies have been observed in rheumatoid arthritis (RA). Notably, antibodies targeting both MAA and citrullinated (CIT) modified proteins are associated with the development of rheumatoid arthritis associated interstitial lung disease (RA-ILD), a leading cause of death among RA patients. In addition, MAA and citrullinated (CIT) adducts are enriched and co-localized in the joints and lungs of RA patients. These MAA and CIT modified fibrinogen (FIB) antigens were shown to activate macrophages, exacerbating pro-inflammatory and pro-fibrotic responses that may contribute to RA-ILD development. However, it remains unclear whether varying levels of MAA modification on proteins elicit differential macrophage responses. We hypothesize that the extent of MAA modification on FIB differentially influences macrophage activation and their subsequent pro-inflammatory and pro-fibrotic responses.

EXPERIMENTAL DESIGN: Human FIB was MAA modified by incubation with different millimolar (mM) concentrations of malondialdehyde and acetaldehyde. Malondialdehyde:acetaldehyde ratios were as follow: 1:1, 2:1, 4:1, 10:5, 16:8, 20:10, 24:12, and 32:16. FIB was citrullinated by incubating with rabbit peptidyl arginine deaminase-2 (PAD2) enzyme. For dual modifications, FIB was first MAA modified and then citrullinated.

U937 human monocytes were differentiated into macrophages using PMA. Macrophages were stimulated with either unmodified FIB (FIB), MAA-modified FIB (FIB-MAA), citrullinated FIB (FIB-CIT), or MAA-CIT dually modified FIB (FIB-MAA-CIT). Two days after stimulation, supernatants were collected, and PDGF and IL-1β were measured by ELISA.

RESULTS: MAA-CIT dually modified FIB elicited greater macrophage activation than single modification alone. However, the extent of MAA modification on FIB significantly influenced the macrophage response. Following MAA-CIT stimulation, the secretion of the pro-fibrotic marker, PDGF was highest when MAA modification was at ratios between 4:2 and 10:5 ratio, where the secretion of the pro-inflammatory cytokine IL-1β peaked when MAA modification ratios were at 10:5 or higher.

CONCLUSION: Macrophage signaling following MAA-CIT stimulation is dependent on the concentration of MAA adducts. Specific concentrations of the MAA adduct trigger both pro-inflammatory and pro-fibrotic responses, while other concentrations predominantly drive either pro-inflammatory or pro-fibrotic response alone. Further research is needed to determine the physiological concentration of MAA adducts during different stages of RA, which may provide insights into the pathophysiology of RA and its complicatio

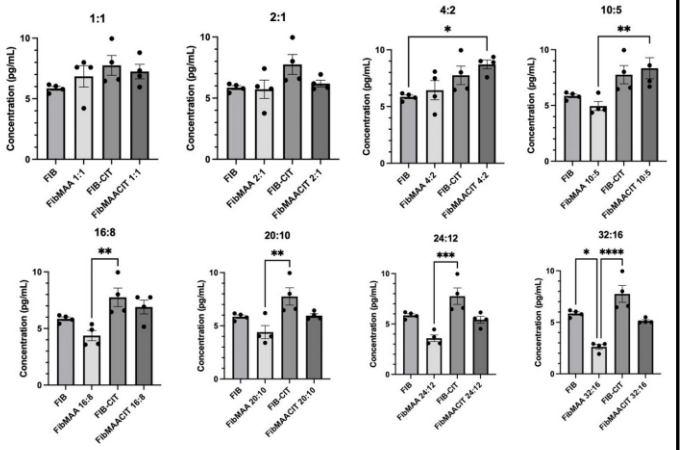

Figure 1. PDGF secretion from U937 macrophage following stimulation with MAA and/ or CIT modified FIB. Ratio of malondialdehyde:acetaldehyde (in mM) used for MAA modification was shown on top of each graph. *p<0.05, **p<0.01, ***p<0.001, ****p<0.0001

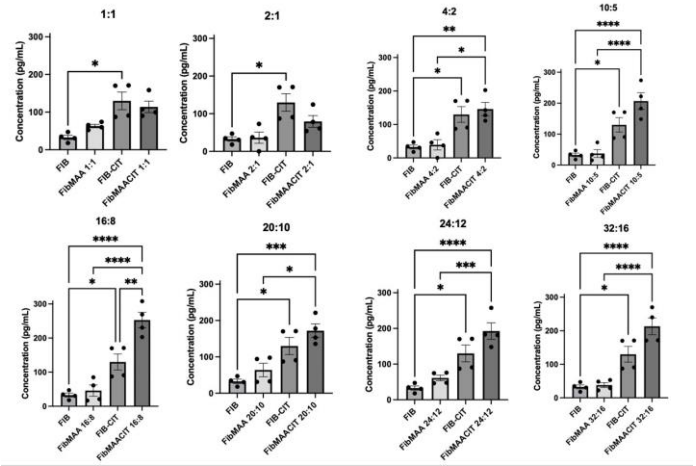

Figure 2. IL-1β secretion from U937 macrophage following stimulation with MAA and/or CIT modified FIB. Ratio of malondialdehyde:acetaldehyde (in mM) used for MAA modification was shown on top of each graph. *p<0.05, **p<0.01, ***p<0.001, ****p<0.0001

CO-MODIFICATION OF CITRULLINATED PROTEINS WITH MALONDIALDEHYDE-ACETALDEHYDE LEADS TO AMPLIFIED T CELL RESPONSES AND INCREASED DISEASE-SPECIFIC AUTOANTIBODY CONCENTRATIONS

Breanna M. Butler, Wenxian Zhou, Michael J. Duryee, Nozima Aripova, Engle E. Sharp, Carlos D. Hunter, Bridget Kramer, Harlan R. Sayles, James R. O'Dell, Geoffrey M. Thiele, Bryant R. England, and Ted R. Mikuls (UNMC Omaha, NE)

***Background*:** Anti-citrullinated protein antibody (ACPA) is highly specific to rheumatoid arthritis (RA). Beyond citrullination, other post-translational protein modifications including malondialdehyde-acetaldehyde (MAA) are targeted by T cells and autoantibodies in RA. MAA is abundant in RA synovial tissues and strongly co-localizes with both citrulline and B cells, suggesting that MAA expression could modulate adaptive immune responses to citrullinated proteins. In this study, we quantified changes in T cell responses and autoantibody reactivity resulting from co-modification of a citrullinated protein with MAA.

Significance of problem: T cell responses in RA are responsible for the initiation of antibody production and play a significant role in the pathogenesis of RA. However, little is known about the mechanism behind how T cells respond to post-translationally modified RA antigens.

Hypothesis: Fibrinogen modified with both MAA and CIT generates a more robust T cell response compared to a single post-translational modification.

***Experimental Design*:** Peripheral blood mononuclear cells (PBMCs; n=10) and serum (n=2484) were collected from RA participants in the Nebraska Rheumatology Biobank (NRB) and Veterans Affairs Rheumatoid Arthritis Registry (VARA), respectively. PBMCs (NRB) were isolated and stimulated with citrullinated fibrinogen (FIB-CIT), MAA-modified FIB (FIB-MAA), or co-modified FIB (FIB-MAA-CIT) for 48 hours, followed by incubation with autologous T cells and evaluated for: 1) T cell proliferation using IFN-γ ELISpot kits; or 2) Th1, Th2, T-Reg, and Th17 cell types by flow cytometry. ELISpot and flow cytometry data were analyzed using one-way ANOVA with Tukey's multiple comparison test. Serum levels (relative units) of IgG antibody to FIB-CIT, FIB-MAA, and FIB-MAA-CIT were quantified via ELISA (VARA). Antibody positivity was established as >2 SD above mean levels quantified in a separate cohort of 103 healthy controls. Seropositivity to modified and co-modified fibrinogen was compared by chi-square tests.

***Results/Data*:** Participant characteristics were similar in the 2 cohorts (90-91% male; mean age 63-73 years; 78-100% anti-CCP positive). CD4 cells proliferated significantly more to FIB-MAA-CIT than either FIB-CIT or FIB-MAA ($p<0.01$) (**Fig. 1A**). This proliferation represented a predominant Th2 response based on increased GATA3 %-positivity in response to FIB-MAA-CIT vs. FIB-CIT or FIB-MAA ($p<0.0001$) (**Fig. 1B**). In contrast, Th1 (CD183) (**Fig. 1C**), T-Reg (CD25) (**Fig.1D**) and Th17 (STAT3) %-positivity (**Fig. 1E**) showed no differences between FIB-CIT, FIB-MAA, and FIB-MAA-CIT. In VARA, the proportion of participants positive for serum IgG antibodies to FIB-CIT (68%) was significantly greater than positivity for either FIB-MAA-CIT (43%) or FIB-MAA (0.6%) ($p<0.0001$) (**Fig. 2**).

***Conclusions*:** These results demonstrate that co-modification of CIT-protein with MAA significantly amplifies CD4 T cell proliferation and promotes a Th2 response to antigen stimulation. Given the known role of Th2 cells in promoting autoantibody expression, our data further suggest that resulting T cell responses promote the generation of ACPA but not anti-MAA antibody. **Figure 3** provides a summary of the hypothesis for the mechanism behind these results. Additional investigation is needed to understand whether these observations are driven by linked recognition (binding and uptake of co-modified antigen followed by preferential processing and presentation of CIT antigen) and whether interventions targeting MAA could reduce pathologic immune responses to CIT-protein in RA.

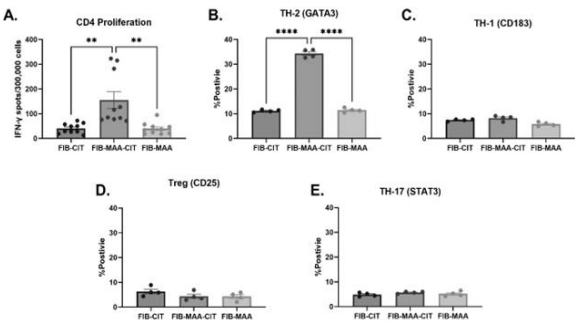

Figure 1. CD4 Proliferation and Percent Positivity of T Cell Phenotypes in Response to Modified Fibrinogen

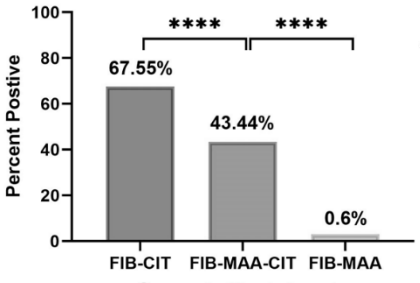

Figure 2. Serum IgG Antibody Levels to Modified Fibrinogen

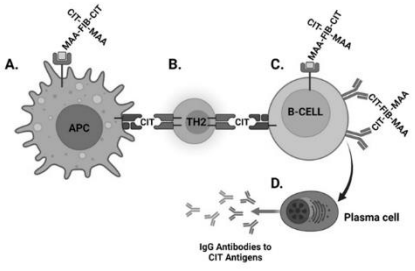

Figure 3. Potential Mechanism by which Co-modification of a Protein with MAA and CIT Amplifies Both the T cell and Antibody Responses to CIT

VULVAR SQUAMOUS CELL CARCINOMA DEMOGRAPHICS: A NCDB STUDY

Elizabeth Byrne [a]; Mya Hendry [a]; Grace Folino [a]; Peter Silberstein [a]; Marco DiBlasi [a]

a. Creighton University School of Medicine, Omaha, Nebraska, USA

Background

Vulvar squamous cell carcinoma (VSCC) is the dominant malignancy of the vulva, accounting for 95% of malignant tumors in the vulva, and 6% of female reproductive cancer overall. Current literature suggests that age, race/ethnicity, and geographic location are correlated with variance in VSCC incidence rates and clinical outcomes.

Significance

The impact of demographic and prognostic profiles on overall survival (OS) rates of VSCC, as demonstrated by this study, emphasizes the need for individualized care plans with consideration of patient demographics to fully understand the population this cancer affects.

Hypothesis, Problem, or Question

This study aims to investigate the underlying demographic or prognostic factor disparities amongst the VSCC patient population.

Experimental Design

This study is a retrospective analysis of the National Cancer database (NCDB) from 2007 to 2021. Patients were identified using specified ICD-10 diagnosis codes for malignant neoplasm of the vulva, as well as histology codes for squamous cell carcinoma of the vulva, and grade III or high grade squamous intraepithelial neoplasia. Demographic and prognostic factors such as age, race/ethnicity, facility type, geographic location, insurance status, education level, income, Charles-Deyo Comorbidity Score, histology, tumor grade, cancer staging, and distance traveled for healthcare were correlated with survival times.

Results/Data

After filtering NCDB data for inclusion criteria, the final total patient population size was 58,732 patients. The number of cases of VSCC per year increased from 2007 to 2021 (3409 and 4170, respectively). The mean age of diagnosis was 64.15 years old (std. Deviation of 15.076). Of the cases analyzed, the majority were White (88.31%), Non-Hispanic/Non-Spanish (92.70%), insured by Medicare (50.17%), with a median income between $48000 to $62999 (23.73%), and were located in the South Atlantic region (20.54%). Most cases were seen at Academic/Research Programs (38.43%), with 7.0% to 12.9% of patients having a high school degree (28.96%) and an average comorbidity Charles-Deyo Score of 0.44. General Squamous Cell Carcinoma was the most frequent histology reported (99.5%), and most patients presented with Stage 1 VSCC (44.2%). Prognostic factors resulting in better overall survival included lower Charles-Deyo Score ($p<0.001$), histology type of Vulvar Intraepithelial Neoplasia, Grade III ($p\geq0.001$), being of Black race ($p<0.001$ against White; $p<0.040$ against Other races), going to a Academic/Research Program ($p<0.001$, CI 95% [109.263, 111.826), insured by Private Insurance ($p<0.001$, CI 95% [146.217, 148.648]), a median income over $63,000 ($p<0.001$ compared to a median income less than $38,000 and income between $38,000 and $47,999; $p=0.008$ compared to median income between $48,000 and $62,999, CI 95% [113.706, 116.911]), and no lymph node involvement ($p<0.001$, CI 95% [123.254, 126.050]).

Conclusions

Identifying these demographic influences on survival has revealed disparities amongst the VSCC population, and will hopefully serve as a valuable tool to characterize prognostic factors.

CLINICAL UTILITY OF THE BIOFIRE PNEUMONIA PANEL IN THE DIAGNOSIS AND TREATMENT OF PNEUMONIA AMONG SOLID ORGAN TRANSPLANT PATIENTS.

Ryan C. Chapman, Trevor C. Van Schooneveld, Sias Scherger, Andre C. Kalil, Carlos A. Gomez (University of Nebraska Medical Center, Omaha, NE)

Background, Significance, and Hypothesis: Solid-Organ Transplantation (SOT) patients are at increased risk for pneumonia, and severe outcomes such as hospitalization, ICU admission, and mortality. The etiology of pneumonia varies according to risk factors and geography. Conventional cultures of respiratory specimens (e.g. sputum, bronchoalveolar lavage) are the gold-standard for pathogen identification. However, these methods have low sensitivity and may be affected by prior antimicrobials. Molecular methods such as multiplex PCR panels have rapid turnaround time and high sensitivity. Herein, we sought to evaluate the diagnostic performance of the BioFire FilmArray Pneumonia Panel (BFAPP), a multiplex PCR panel, and its impact in antimicrobial utilization and clinical outcomes in SOT patients at the University of Nebraska Medical Center (UNMC).

Experimental Design: We reviewed BFAPP panel results from April 2020 to June 30, 2024, collected at the Nebraska Medicine microbiology lab. Patients who underwent SOT prior to BFAPP were included. Demographic, clinical, laboratory, radiographic, and outcomes data were collected via REDCap. Descriptive statistics were performed.

Results: Out of 6203 unique BFAPP results in 4008 patients, 998 panel results were performed in 386 SOT-patients (positivity rate: 35%). A single target was detected in 226/350 (64.5%): 159 (45.4%) bacteria and 67 (19.1%) respiratory viruses. In 126 cases (35%), BFAPP found ≥2 targets: 64 (18%) detected ≥2 bacteria, 4 (1.14%) detected ≥2 viruses, and 56 (16%) were mixed flora (≥1 bacteria and ≥1 virus) (**Table 1**). The most frequently identified single bacteria and virus were *Pseudomonas aeruginosa* and Rhinovirus/Enterovirus, respectively. However, combined MSSA and MRSA were more common than *P. aeruginosa*.

Conclusion and Future Directions: Bacteria predominated over viruses, with *P. aeruginosa, S. aureus and H. influenzae* being most common. Gram-negative rods were predominant among the top 10 targets (70%). Detection of 2 or more pathogens was common (36%), including mixed infections (16%). To date, this study has the largest population of SOT patients tested with the BFAPP for community and hospital-acquired pneumonia. We plan to investigate the panel's performance compared with conventional testing and its impact on antimicrobial prescription, time to de-escalation, duration of therapy, and clinical outcomes.

Table 1: The number of positive and negative BFAPP results collected for SOT patients at UNMC between May 2020 and June 2024.

BFAPP results	Amount N (%)
Positive	350 (35%)
Single Organism -Bacteria -Virus	226 (64.5%) 159 (45.4%) 67 (19.1%)
Multiple Organisms -Bacteria only -Virus only -Mixed Flora	124 (35%) 64 (18%) 4 (1.14%) 56 (16%)
Negative	648 (65%)
Total	998

Footnote: Mixed flora refers to at least one bacterial and one viral target positive in a single run.

CHLOROTOXIN FRAGMENTS BIND TO NEUROPILIN-1 AND INHIBIT GLIOBLASTOMA CELL MIGRATIOIN

Meron Demeke, Sándor Lovas (Creighton University, Omaha, NE)

Background, Significance, Hypothesis: Glioblastoma, the most prevalent malignant brain tumor, poses a challenge in treatment due to its rapid growth and aggressive nature. Chlorotoxin (Ctx), a 36 amino acid residue peptide from the venom of *Leiurus quinquestriatus* scorpions, has emerged as a promising drug candidate for therapeutic use. Ctx has been shown to selectively bind to glioblastoma cells and inhibit glioblastoma cell migration[1]. Several protein targets of Ctx have been proposed, including Neuropilin-1 (NRP-1)[2]. NRP-1 is a transmembrane receptor that plays an important role in angiogenesis and tumor progression. A previous study determined that the C-terminal fragment of Ctx (residues 27-36) retains its bioactivity and can inhibit glioblastoma cell migration as effectively as the full-length Ctx[3]. This finding prompted us to investigate further modifications we can make to the C-terminal region of Ctx to elicit a stronger effect on inhibiting glioblastoma cell migration. This lead us to our working hypothesis that Ctx, along with our designed C-terminal fragments, bind to NRP-1 and inhibit glioblastoma cell migration.

Experimental Design: C-terminal Ctx fragments were designed by modifying the disulfide bridges that stabilize its structure. Designed fragments were *N*- and *C*-terminally acetylated and amidated, respectively. The first peptide, P75, corresponds to Ctx residues 24-36 and includes a disulfide bridge between residues Cys^{28} and Cys^{33}. The Cys^{35} residue was substituted with a Ser residue, resulting in the sequence of Ac-GRGKCYGPQCLSR-NH_2. The second peptide, P78, corresponds to Ctx residues 27-34. P78 includes a disulfide bridge between residues Cys^{28} and Cys^{33}, with the sequence of Ac-KCYGPQCL-NH_2. Cell migration inhibition assays were performed using the U-87 MG glioblastoma cells. Binding interactions between the synthetic peptides and recombinant NRP-1 were assessed by measuring changes in melting temperature of the protein and the protein − peptide complexes using nano differential scanning fluorimetry (nanoDSF), as well as measuring binding affinity using surface plasmon resonance (SPR) methods.

Data and Results: P78 demonstrated statistically significant inhibition of glioblastoma cell migration compared to that of the untreated control cells. P78 showed greater efficacy than full-length Ctx in the cell migration inhibition assay. Both NanoDSF and SPR measurements showed that both peptides display concentration-dependent melting temperature shifts and binding affinities in high micromolar ranges.

Conclusion: The results support the hypothesis that the C-terminal fragments of Ctx bind to NRP-1 and inhibit glioblastoma cell migration. The enhanced efficacy of P78 compared to the full-length Ctx underscores the potential for optimizing the structure of C-terminal fragments to enhance their bioactivity for their potential use as therapeutic tools.

---

1 *Lyons SA, O'Neal J, Sontheimer H.* Chlorotoxin, a scorpion-derived peptide, specifically binds to gliomas and tumors of neuroectodermal origin. Glia. 2002 Aug;39(2):162-73. doi: 10.1002/glia.10083. PMID: 12112367.
2 *Farkas S, et al.* Chlorotoxin binds to both matrix metalloproteinase 2 and neuropilin 1. J Biol Chem. 2023 Sep;299(9):104998. doi: 10.1016/j.jbc.2023.104998. Epub 2023 Jun 30. PMID: 37394009; PMCID: PMC10477481.
3 *Dastpeyman M, et al.* A C-Terminal Fragment of Chlorotoxin Retains Bioactivity and Inhibits Cell Migration. Front Pharmacol. 2019 Mar 20;10:250. doi: 10.3389/fphar.2019.00250. PMID: 30949052; PMCID: PMC6435586.

A NOVEL SMALL MOLECULE TREM1 INHIBITOR AS POTENTIAL TREATMENT FOR GLOBAL ISCHEMIA-INDUCED NEUROINFLAMMATION AND NEURONAL DEATH

Adya Dhuler[1], Hyunha Kim[1], Prerna Tiwari[1], Rachael Urquhart[1], Gopal Jadhav[1], Jee-Yeon Hwang[1]

[1] Department of Pharmacology and Neuroscience, Creighton University School of Medicine, Omaha, NE, USA

Background
Over 200,000 Americans suffer from global cerebral ischemia annually- most often from cardiac arrest- with persisting cognitive deficits or death. Current emergency treatments for cardiac arrest focused on restoring cardiac function and blood flow have increased survivor rates but fail to address neurodegeneration and cognitive deficits, leading to debilitating neurological defects in survivors, presenting an unmet medical need. Global ischemia leads to selective, delayed death of hippocampal CA1 pyramidal neurons, causing severe cognitive deficits. These neurological deficits are closely associated with transcriptional changes in this vulnerable brain region.

Preliminary Studies
In preliminary studies, the 4-VO rat model for ischemia induction had selective, delayed neuronal death in hippocampal CA1 pyramidal neurons, with cognitive deficits confirmed via behavioral testing (e.g., Barnes Maze, NOR). Subsequent RNA-seq using next-generation Massively Parallel Sequencing was performed to investigate gene expression alterations in post-ischemic hippocampal CA1 in rats. With Ingenuity Pathway Analysis (IPA), 'Neuroinflammation' and 'Triggering receptor expressed in myeloid cells 1 (TREM1) signaling' are the primary altered canonical pathways. This was confirmed by increased TREM1 and DAP12 expression 24–48 hours post-ischemia in RT-qPCR and Western Blot. TREM1 likely amplifies inflammation via cytokine secretion and transcription factor activation (NF-kB, STAT3), leading to neuronal death. LR12, a TREM1 peptide inhibitor, reduced neuronal loss in the hippocampal CA1 following global ischemia in rats. Taken together, these findings suggest that TREM1 activation is critical to neuronal death and inhibition of TREM1 can be a therapeutic strategy for global ischemia.

The goal of this study: Despite of efficacy, current TREM1 inhibitor including LR12 has limitations such as poor cell permeability and rapid degradation. To address these issues, we recently developed a novel small-molecule TREM1 inhibitor, GJ079, using molecular docking techniques. In this study, we determine neuroprotective effects of GJ079 in global ischemia.

Methods and Results
In male rats, A single 500ng dose of GJ079 was administered via stereotaxic injection the day before the induction of ischemia using the 4-vessel occlusion (4-VO) model. Histology with Toluidine blue staining showed that GJ079 significantly attenuated ischemia-induced neuronal death in hippocampal CA1 7 days following ischemia. Whereas Immunolabeled Iba-1 (microglia) and GFAP (astrocytes) were increased after global ischemia indicating activation of neuroinflammation, administration of GJ079 rescued these events at 7 days after ischemia. In addition, immunolabeling of M1 microglia marker CD86 and M2 microglia marker CD 206 was increased in response to global ischemia. GJ079 treatment rescued an increase in CD86 but not CD206, suggesting that GJ097 protects neurons via attenuating proinflammatory microglial (M1) activation. At 3 days after ischemia, GJ079 preserved neuronal marker MAP2 and synaptic marker PSD-95, indicating synaptic protection. Moreover, qPCR analysis of hippocampal CA1 showed GJ079 significantly decreased global ischemia-activated proinflammatory cytokines IL-18 and IL-6, and the downstream factors of TREM1, NF-κB and STAT3, indicating that GJ079 prevents TREM1-signalying pathway.

Conclusion
By reducing the expression of proinflammatory cytokines, GJ079 treatment modulates TREM1 signaling pathways to mitigate neuroinflammation and neuronal loss and preserve synaptic integrity in the CA1 region. It consequently demonstrates significant neuroprotective effects of GJ079 in global cerebral ischemia highlighting its potential as a novel therapeutic approach for ischemia-induced cognitive deficits and other clinical conditions associated with neuroinflammation, neuronal death, and cognitive impairment.

CHARACTERIZATION OF SNARL TYPES IN HEALTHY INDIVIDUALS: ESTABLISHING A COMPARATIVE BASELINE FOR FACIAL PARALYSIS

Janani Raman, Maya Samuel, Jenna Lehn, Carissa Besonen, Vikram Murugan, Rahul Varman, Marco DiBlasi
(Creighton University, Omaha, NE)

Background, Significance, Hypothesis: Facial synkinesis creates functional limitations that may affect an individual's ability to eat, speak, or express emotion accurately, resulting in negative self/social perceptions. Individuals with non-flaccid facial paralysis often exhibit a snarl expression when they attempt to smile and undergo selective denervation surgery to fix aberrant nerve regrowth. There is a lack of literature classifying the underlying mechanism and muscular involvement behind the snarl expression in healthy individuals. This study analyzes the snarl in healthy individuals to create a clinically useful comparative baseline for patients suffering from facial paralysis. The results will guide clinicians with developing an efficacious treatment plan for patients with facial paralysis.

Experimental Design: 50 healthy participants were selected (25 male and 25 female) and pictures were taken of their faces at rest, performing a right and left unilateral snarl, and bilateral snarl, and smiling. The resting face represents the negative control and the smiling face represents a positive control for happiness. Demographic data was collected from all participants. Using Adobe Photoshop, Clinician Facial Assessment was performed on every facial expression, evaluating brow elevation, nasolabial fold severity, nasal deviation, nasal tip mid-glabella distance, alar base asymmetry, alar base elevation, margin reflex distances (MRD) 1 and 2, intercommissure distance, commissure elevation, upper and lower lip movements, glabellar distance, lip shape, and glabellar shape. Pictures were then evaluated using the Python based software, Emotrics, to automatically compute facial metrics. Lastly, Noldus FaceReader's software was used to assay facial expressions for various levels of emotions.

Data/Results:
In evaluating the unilateral and bilateral snarl expressions compared to the resting facial position, the Clinician Facial Assessment's findings included: increased nasolabial fold severity rating on the ipsilateral side for unilateral snarls and on both sides for bilateral snarls, increased nasal deviation for unilateral snarls, decreased nasal tip mid-glabella distance for both unilateral and bilateral snarls, increased alar base elevation for both unilateral and bilateral snarls, decreased MRD1 and MRD2 on the ipsilateral side for unilateral snarls and on both sides for bilateral snarl, increased intercommissure distance, increased commissure elevation for unilateral snarls, increased lip movement for both snarls, and decreased glabellar distance for both snarl types. These patterns were confirmed with Emotrics software. Using FaceReader software, snarl patients had significantly increased conveyance of disgust than resting and smiling expressions. Additionally, snarl expressions retained an increased percentage of happiness compared to resting and increased levels of scared compared to resting.

Conclusions:
The findings concluded by this study provide a neuromuscular framework of how facial paralysis can present, thus highlighting what specific facial structures should be treated to restore normal facial expressions. Additionally, it is important to note that patients affected by facial paralysis and exhibiting a snarl expression when attempting to smile will be perceived as unintentionally displaying disgust and scared emotions to others. Lastly, an interesting finding is that while a snarl is still being displayed, there are significantly detectable levels of happiness as the patient is still trying to smile.

MODULATION OF KINASE SIGNALING BY APLP2 IN PANCREATIC CANCER CELLS

Kenadie R. Doty, Kaitlin J. Smith, Gabrielle L. Brumfield, Joyce C. Solheim (UNMC, Omaha, NE)

Background and Significance: Pancreatic cancer is one of the most aggressive and fatal malignancies, with a five-year survival rate of only 13%. Its poor prognosis stems from late diagnosis, rapid progression, and limited treatment options, underscoring the urgent need for a deeper understanding of the disease. Kinase signaling pathways, which regulate essential cellular processes such as proliferation, survival, and metastasis, are frequently dysregulated in pancreatic cancer, significantly contributing to its development and progression. Understanding the molecular mechanisms governing these pathways is critical for identifying therapeutic targets, developing predictive biomarkers, and personalizing treatments to improve outcomes for patients facing this devastating disease. Overexpression of amyloid precursor-like protein 2 (APLP2) in pancreatic cancer suggests that it may promote cancer progression. Despite this, the specific mechanisms by which APLP2 may influence critical kinase signaling pathways in pancreatic cancer remain undefined, revealing a gap in knowledge that justifies further investigation. This research aims to address this gap by examining the phosphorylation profiles of kinases and their substrates to uncover how APLP2 influences pancreatic cancer signaling and identify the molecular pathways it modulates.

Hypothesis: APLP2 modulates kinase signaling pathways in pancreatic cancer cells by influencing phosphorylation events that are essential for tumor progression and cellular mechanisms underlying cancer cell activity.

Experimental Design: To investigate the role of APLP2 in kinase signaling pathways in pancreatic cancer, we used S2-013 human pancreatic cancer cells. APLP2 was downregulated via transient transfection with ON-TARGETplus SMARTpool siRNA, while non-targeting scramble siRNA served as a control. Knockdown efficiency was confirmed by Western blot analysis. Kinase signaling was assessed in the APLP2 knockdown and control cells using the Proteome Profiler™ Human Phospho-Kinase Array, a membrane-based immunoassay that quantifies phosphorylation levels of 37 kinases and their protein substrates. Differentially phosphorylated kinases were analyzed using Qiagen Ingenuity Pathway Analysis (IPA) to identify enriched pathways linked to APLP2-mediated signaling, offering insights into the affected signaling pathways.

Data and Results: Western blot analysis confirmed a reduction in APLP2 expression, validating the efficiency of siRNA transfection (Fig. 1). The phospho-kinase array showed significant changes in kinase signaling pathways after APLP2 knockdown (Fig. 2). Specifically, APLP2 knockdown led to a 2.375-fold increase in phosphorylation of proline-rich Akt substrate of 40 kDa (PRAS40), and significant decreases in phosphorylation of cAMP response element binding protein (CREB), extracellular signal-regulated kinase 1/2 (ERK1/2), and c-Jun N-terminal kinases 1/2/3 (JNK 1/2/3). To further interpret the biological relevance of these changes, Qiagen IPA was used to map the interactions between the kinases significantly affected by APLP2 knockdown. The network analysis revealed three major signaling pathways impacted by modulation of APLP2 expression: (1) Mitogen-activated protein kinases (MAPK) targets and nuclear events mediated by MAPK, (2) G-protein coupled receptor signaling, and (3) focal adhesion kinase (FAK) signaling.

Conclusion: These results reveal that APLP2 knockdown significantly alters key kinase signaling pathways in pancreatic cancer cells, particularly those involved in MAPK, G-protein-coupled receptor, and FAK signaling. Notably, the decrease in JNK and ERK phosphorylation and the increase in PRAS40 phosphorylation highlight APLP2's potential role in modulating critical pathways that drive pancreatic cancer progression. These results provide valuable insights into the molecular mechanisms underlying APLP2's impact on kinase signaling and suggest its involvement in pathways that regulate cell survival and proliferation. Future research will focus on validating these findings using additional pancreatic cancer models and kinase inhibitors to further elucidate APLP2's role and explore its potential as a therapeutic target in pancreatic cancer.

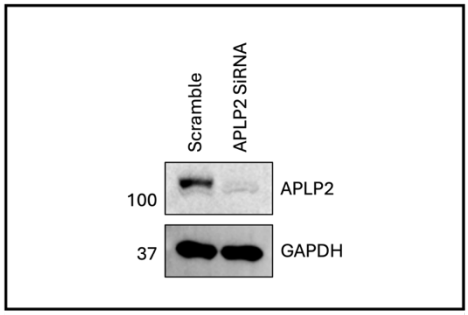

Figure 1: Western blot confirmation of APLP2 knockdown in S2-013 cells.

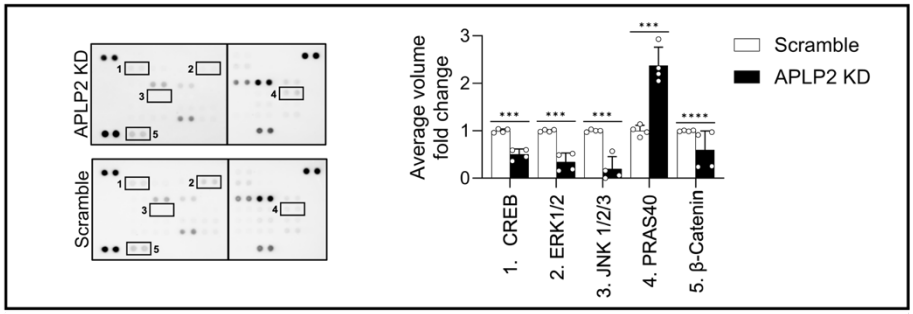

Figure 2: APLP2 knockdown alters phosphorylation of key signaling proteins in S2-013 cells. (Left) Phospho-kinase array images of APLP2 knockdown and scramble controls. (Right) Bar graph depicting fold changes in average volume, representing relative phosphorylation levels. Statistical significance was assessed with an unpaired t-test; ***p<0.001, **** p<0.0001.

ALCOHOL REDUCES CIRCULATING LEVELS OF LIVER-EXPRESSED ANTIMICROBIAL PEPTIDE (LEAP2): PUTATIVE ROLE IN ALCOHOL-ASSOCIATED LIVER DISEASE

Ojeshvi Ethiraj, Sundararajan Mahalingam, Ramesh Bellamkonda, Carol A. Casey, Kusum K. Kharbanda, and Karuna Rasineni (UNMC Omaha, NE)

Background, Significance and Hypothesis: The liver sustains the greatest degree of tissue injury by chronic heavy drinking which causes a wide spectrum of pathology, the most characteristic of which are steatosis, hepatitis, and fibrosis/cirrhosis. Pathophysiological mechanisms involved in development and progression of alcohol-associated liver disease (ALD) are complex and multifactorial, including gut, pancreas and adipose tissue dysfunction and altered organ crosstalk. Recent research from my laboratory has established that alcohol-induced alterations in circulating gut peptide hormone level perturb organ crosstalk and promote liver injury. Specifically, we have shown that alcohol-induced increases in serum levels of stomach-derived ghrelin impairs insulin secretion from pancreatic β-cells. The consequent reduction in the circulating insulin levels promotes adipose lipolysis and mobilization of fatty acids to the liver, ultimately contributing to the development of hepatic steatosis. We have further shown that inhibiting ghrelin-ghrelin receptor interaction prevents ALD development. A recently discovered predominantly liver and intestine-expressed peptide named liver-expressed antimicrobial peptide 2 (LEAP2) is an allosteric inhibitor of the ghrelin receptor and noncompetitively reduces the magnitude of the detrimental effects of ghrelin. The goals of this study were (i) to explore the status of LEAP2 expression and levels in clinical samples and in animal models of ALD and (ii) to examine the function and regulators of LEAP2 in the context of ALD (iii) to check the level of LEAP2 secreted in mouse intestinal organoids. Chronic alcohol consumption disrupts metabolic and microbial homeostasis, leading to reduced levels of LEAP2. This reduction impairs LEAP2's protective roles in inhibiting ghrelin receptor signaling and maintaining antimicrobial defenses, exacerbating liver injury. We hypothesize that restoring LEAP2 levels can counteract these detrimental effects, providing a potential therapeutic approach to mitigate the progression of alcohol-associated liver disease.

Experimental Design: Male Wistar rats were pair-fed with Lieber-DeCarli ethanol or control liquid diets for 7 weeks. Serum and liver tissue samples were collected for biochemical analyses, including ELISA to quantify LEAP2 levels. Hepatocytes were isolated from chow-fed rats and cultured with glucose, insulin, oleic acid, or ghrelin to evaluate LEAP2 secretion and expression. De-identified human serum and liver tissue samples from normal, alcoholic hepatitis, and cirrhotic patients were obtained from biobank resources. Additionally, mouse small intestinal crypts were isolated and cultured as organoids in Matrigel. Media collected from primary and secondary organoid cultures were analyzed for LEAP2 secretion.

Data and Results: Ethanol-fed rats exhibited significantly lower serum LEAP2 levels compared to controls. Similar reductions were observed in patients with alcoholic hepatitis and cirrhosis, where hepatic LEAP2 protein content was markedly decreased. Glucose and insulin treatments increased LEAP2 expression and secretion in primary hepatocytes, while oleic acid and ghrelin suppressed LEAP2 levels. In vitro assays demonstrated that LEAP2 attenuates bacterial overgrowth, indicating its antimicrobial potential. Mouse intestinal organoids were found to secrete LEAP2 into the culture medium, supporting its role in gut-liver axis signaling.

Conclusion: Our studies indicate that the alcohol-induced increased free fatty acid & ghrelin circulating levels and decreases in serum insulin levels may be responsible for the reduction in LEAP2 levels seen in patients and animal models of ALD. This decrease in the circulating levels of the protective LEAP2 could have several detrimental functional ramifications via the reduction in ghrelin receptor antagonism and antimicrobial effect to promote the initiation and progression of ALD.

Figures (A) & (B) Ethanol administration results in increased serum ghrelin and decreased serum LEAP2 levels in rat

Figure (C) LEAP2 levels in controls and patients with ALD

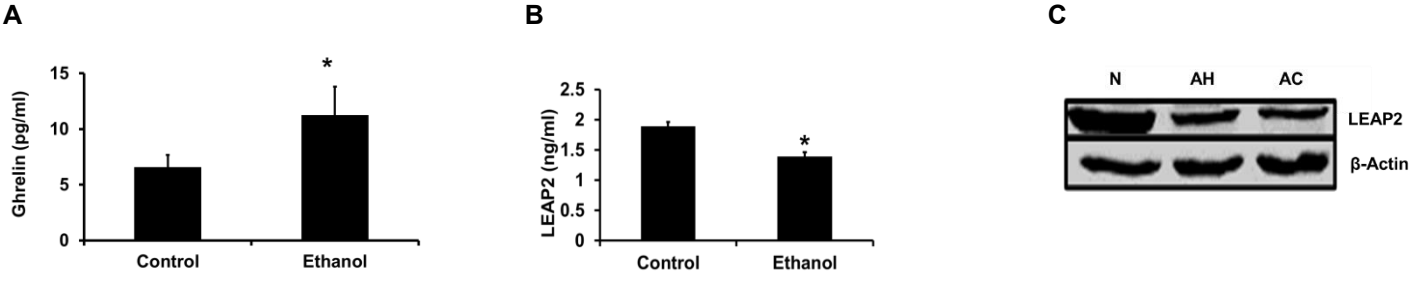

Figures (A) Serum ghrelin and **(B)** Serum LEAP2 levels in control and ethanol-fed rats. Values are mean ± SEM (n=8); *p<0.05 indicates statistical significance.
Figure (C) Western blot showing hepatic LEAP2 protein content in representative normal (N), alcoholic hepatitis (AH) & alcohol-associated cirrhotic (AC) patients. Values are mean ± SEM (n= 6); *p ≤ 0.05.

DIFFERENCES IN LABOR AND DELIVERY OUTCOMES BY PATIENT LANGUAGE

Grace Folino [a]; Kallin Hermann [a]; Megan Kalata [b]

a. Creighton University School of Medicine, Omaha, Nebraska, USA
b. CHI Health, Omaha, Nebraska, USA

Background:
With increasing diversity among patients' primary language, there has become an increasing need to understand the importance of language proficiency in patient experience. Current literature demonstrates that language barriers compromise the quality and satisfaction of patient care, increase perceived discrimination, and create risk for lack of informed consent. In environments such as Labor and Delivery (L&D), incomplete communication due to language discordance may be related to increased adverse events.

Significance of Problem:
The association of language discordance and adverse healthcare experiences underscores the importance of evaluating obstetric care events between patients with a primary language other than English and patients with a primary language of English. Omaha's diverse language makeup necessitates understanding maternal language discordance to better address patient experiences and outcomes.

Hypothesis, Problem, or Question:
This study aims to investigate if a difference exists in maternal outcomes for patients with a primary language other than English (NEPL) and patients with a primary language of English (PLE).

Experimental Design:
Participants who had a delivery at Creighton University Medical Center - Bergan Mercy Hospital between June 2020 and June 2024 were screened for eligibility. Maternal demographic variables and those pertinent to pregnancy were collected. L&D events were categorized into mode of delivery, delivery complication, NICU admission, vacuum or forceps delivery, antibiotic course for mother, steroid course for mother, interpreter use, and diagnosis of gestational diabetes. Demographic variables were stratified by primary language (English vs. non-English). Categorical variables were compared using Chi-Squared tests, and continuous data was compared using Mann Whitney U-test and linear regression. Linear regression models were used to compare differences in mode of delivery.

Results/Data:
A total of 11,935 participants were included. Of these participants, primary language rates were identified as English [75.13%] and non-English [24.9%]. EPL had a significantly higher rate of Cesarean deliveries [26.72%, $p<0.001$] and operative vaginal deliveries [2.5%, $p<0.001$]. NEPL had higher rates of normal spontaneous vaginal delivery [76.21%, $p<0.001$] and breech vaginal delivery [0.13%, $p<0.001$]. NEPL had a lower adjusted odds of a C-section when parity was controlled [19%, $p<0.002$]. There was a significantly higher rate of maternal antibiotic use among EPL [19.55% NEPL; 24.79% PLE, $p<0.001$]. NEPL had a lower rate of both full course steroid administration [NEPL 0.64%; 1.52% PLE, $p<0.001$] and lower rate of partial course steroid administration [NEPL 0.03%; EPL 0.1%, $p<0.001$]. There was a significantly higher rate of NEPL patients that received no steroids at all compared to EPL [NEPL 79.25%; EPL 78.86%, $p<0.001$]. Stage 2 of labor was longer in EPL than NEPL [129.36 minutes and 36.045 minutes, $p<0.001$], and stage 3 of labor was longer in NEPL than EPL [63.964 minutes and 15.263 minutes, $p<0.002$].

Conclusions:
These findings demonstrate differences in L&D events between English and non-English primary languages, prompting the need for targeted interventions to reduce language barriers and mitigate differences in care.

PDK3: A METABOLIC GATEKEEPER OF STEMNESS IN PANCREATIC CANCER STEM CELLS

Neelanjana Gayen, Nivedeta Krishna Kumar, Ayoola O. Ogunleye, Karthik Balakrishnan, Palanisamy Nallasamy, Venkatesh Varadharaj, Marimuthu Saravanakumar, Surinder K. Batra, and Moorthy P. Ponnusamy.

Department of Biochemistry and Molecular Biology, University of Nebraska Medical Center, Omaha, NE.

Background: Pancreatic Cancer (PC) stands as the third highest contributor to cancer-related deaths in the US. Conventional chemotherapy regimens, including gemcitabine and nab-paclitaxel, often show limited success in improving patient outcomes significantly. Recent studies have highlighted the presence of Cancer stem cells (CSCs), which are strongly associated with tumor relapse after initial treatment. This small subpopulation of cells within tumors can survive chemotherapy and radiation, leading to the regeneration of tumors with increased aggressiveness. Their extraordinary metabolic plasticity sets CSCs apart, allowing them to adapt and thrive under various stressful conditions by dynamically switching between different energy sources leading to chemo-resistance, metastasis, and disease recurrence. By identifying key metabolic factors unique to CSCs, researchers can design novel therapeutic strategies that selectively target CSCs while sparing normal tissue. PDK3, a member of the pyruvate dehydrogenase kinase family known to phosphorylate the E1 subunit of the pyruvate dehydrogenase complex (PDHA), resulting in the inactivation of the complex by phosphorylating it, thereby regulating the switch between glycolytic metabolism and mitochondrial oxidation. However, the metabolic characteristics and regulatory mechanisms of CSCs are poorly understood.

Significance: If the current trend in mortality rates for PDAC persists, it is projected to become the second leading cause of cancer-related deaths in the United States by 2030. CSCs, with their unique ability to survive treatment and drive tumor relapse, represent a critical challenge in PC management. Understanding the metabolic reprogramming that sustains CSCs has the potential to disrupt the metabolic adaptations that allow CSCs to survive and propagate tumors could be the key to finally turning the tide against this devastating disease.

Hypothesis: *Pyruvate dehydrogenase kinase3 maintains stemness and distinct metabolic reprogramming in pancreatic cancer stem cells (PCSCs)l and plays a crucial role in the progression of pancreatic cancer.*

Experimental Design/Methods: To test our hypothesis, RNA sequencing was performed on the spheroid-based CSC model to identify metabolic genes uniquely expressed in CSC-enriched populations. We conducted an *in-silico* analysis, to identify potential metabolic targets in PCSCs. Through an *in-vitro* screening process, involving spheroids, flow cytometry-isolated CSCs (Side-Population, CD133+ve), and non-CSCs (Non-Side Population, CD133–ve) we identified PDK3 as the top metabolic factor highly expressed in PCSCs. To explore PDK3's role in pancreatic cancer, we employed two complementary approaches: a lentiviral-mediated shRNA construct targeting PDK3 was stably expressed in PC cell lines, SUIT2 and MiaPaCa2 to assess its direct impact, and a pharmacological inhibition model was utilized to further study PDK3's role in regulating stemness. The effects of PDK3 depletion were analyzed through sphere-formation and colony-forming assays, while flow cytometry was performed to evaluate changes in the stem cell population. Additionally, major glycolytic gene expression was evaluated in PDK3-depleted PCSCs. LC-MS analysis was conducted to elucidate the metabolic pathways influenced by PDK3 in maintaining CSC stemness. Finally, an in vivo study was performed by orthotopically implanting sh-PDK3 PC cell lines and scramble control cells in nude mice to investigate PDK3's role in tumor growth and PCSC maintenance.

Results: In our in-silico analysis of RNA-seq data, PDK3 emerged as one of the 14 overexpressed putative metabolic regulatory genes in CSC populations. Western blotting and qPCR analyses confirmed that PDK3 was significantly overexpressed at both the protein and mRNA levels in spheroid-enriched CSC populations, Side Population (SP) and CD133+ve cells, compared to their non-CSC counterparts (NSP and CD133–ve). Immunohistochemistry (IHC) analysis revealed strong PDK3 expression in human pancreatic ductal adenocarcinoma (PDAC) ($p<0.0001$) and murine (KrasG12D; Pdx-1Cre-KC) tumor sections. Notably, dual-IHC staining demonstrated co-expression of PDK3 with the stemness marker CD44 in human PDAC tissues, underscoring its association with CSC phenotypes. Lentiviral-mediated PDK3 knockdown in SUIT2 and MiaPaCa2 cell lines showed a marked reduction in key glycolytic genes and phosphorylated pyruvate dehydrogenase levels while total PDHA expression remained unchanged indicating PDK3's role in promoting glycolysis in CSCs. Flow cytometry analysis revealed a significant decline in the Side Population, upon PDK3 depletion. Pharmacological inhibition of PDK3 using artesunate impaired stemness-associated traits, reduced sphere-formation, and colony-forming capacities. LC-MS analysis revealed a significant reduction in lactic acid, among other metabolites, upon PDK3 disruption, making it a candidate for further investigation in altered glycolytic flux in CSCs. Orthotopic implantation of PDK3-depleted human PC cell lines in nude mice resulted in significantly reduced tumor growth and weight.

Conclusions and Future Perspectives: Our study highlights PDK3 as a key metabolic regulator in PCSCs, with elevated expression driving glycolytic flux and supporting stemness traits. Further mechanistic studies on PDK3 and analysis of changes in stemness will be performed to establish its role as a potential metabolic regulator in pancreatic cancer.

PATTERNS OF CARE AND TREATMENT OUTCOMES IN ADENOID CYSTIC CARCINOMA OF THE HEAD AND NECK AND OVERALL SURVIVAL

Nicole Grossmann, Ena Wang, Joel Dumonsau, Peter Silberstein, Rahul Varman, Marco DiBlasi (Creighton University School of Medicine Omaha, NE)

Background, Significance, Problem: Adenoid cystic carcinoma (ACC) is a rare malignancy that accounts for just 1% of all head and neck malignancies and 10% of salivary gland cancers. Many patients present with already metastasized disease due to this cancer's predisposed invasive nature. Existing studies of ACC have resulted in a fragmented view due to existing studies utilizing limited data (single-institution populations, narrowly defined populations, and Surveillance, Epidemiology, and End Results (SEER) databases). Due to the rarity of this cancer, analyzing demographics and trends in treatment can help provide stronger and clearer insight for clinicians in regard to earlier diagnosis and shaping individualized treatment strategies for patients.

Experimental Design: Individuals with a confirmed diagnosis of ACC of the head and neck were identified using the National Cancer Database (NCDB) for a retrospective analysis from 2004-2021 (N=12,591). Patient sex, age at diagnosis, race, insurance status, and Charlson-Deyo score were examined by descriptive statistics, while survival was estimated using Kaplan-Meier curves.

Data and Results: After filtering for all inclusion criteria, the final patient population size was 12,591 patients. Of all structures in the head and neck, ACC was most prominent in the salivary glands (45.2%), then gum and other mouth (16.6%), followed by nose, nasal cavity, and middle ear (15.0%), then tongue (5.5%), trachea and upper respiratory tract (4.3%), nasopharynx (3.4%), eye (3.0%), mouth floor (2.2%), larynx (1.7%), lip (1.6%), oropharynx (0.5%), tonsil (0.4%), pharynx (0.3%), hypopharynx (0.2%), thymus (0.1%), and esophagus (0.1%). The number of cases of ACC has slowly increased from 2004 to 2021 with 32.1% of patients being diagnosed at stage IV. Most patients were between 60-79 years old with a mean age of diagnosis of 58.75 years old. The majority of patients were white (78.6%), non-Spanish/non-Hispanic (87.9%), treated in the South Atlantic region (18.1%), and had private insurance (49.3%). 51.9% of patients were in metropolitan areas with a population of 1 million or more. The median distance traveled for treatment was 14.7 miles. 82.8% of patients had a Charlson-Deyo comorbidity score of 0 with a mean Charlson-Deyo comorbidity score of 0.23. 31.4% of patients tested negative for lymph node metastasis, but 56.6% did not have nodes examined. Following surgery, 58.2% of patients received radiation, while 97.1% of patients did not receive palliative care. The median time elapsed from diagnosis before surgery was 14 days. The median time elapsed from diagnosis to treatment (includes surgery) was 20 days. The average survival time was 130.58 months with surgical procedures significantly improving survival time when compared to no surgery. Females had a mean survival of 137.46 months which is longer than males (mean=120.59 months). Of all structures in the head and neck, the lowest overall survival was in the esophagus (mean=52.46 months) while the greatest overall survival was in the gum and other mouth (mean=143.15 months). Patients of Spanish/Hispanic populations lived significantly longer than non-Spanish/non-Hispanic populations (mean=135.428 and 129.333 months, respectively). Other races (mean=147.019 months) survive significantly longer compared to white and black patients (mean=129.825 and 120.348 months, respectively). All forms of insurance (including not insured) provided significantly longer survival than Medicare (mean=95.542 months) as the overall mean was 130.580 months.

Conclusions: This study highlights distinct disparities within the ACC head and neck patient population, with the goal of enhancing physician care and treatment strategies for future cases of ACC.

LOWER PHYSIOLOGICAL LINKAGE WITH CAREGIVERS IS ASSOCIATED WITH WORSE EMOTION RECOGNITION IN PERSONS WITH NEURODEGENERATIVE DISEASES

Anna Haggart, Kuan-Hua Chen, Robert W. Levenson (UNMC, Omaha NE)

Background, Significance and Hypothesis: Persons with neurodegenerative diseases (PWDs) often develop profound cognitive declines as well as impairment in emotional functioning, such as a reduced ability to recognize emotions in others. Recent advances in wearable technology have opened new avenues for studying daily activity in patients with dementia (PWD) outside of the laboratory setting. Wearable devices, such as accelerometers, GPS trackers, and physiological sensors, offer continuous, real-time data collection, which provides a valuable window into the daily lives of PWD. Research utilizing wearable technology in PWD has primarily looked at patterns in sleep, mobility, and exercise monitoring. Studies have shown that wearable devices can effectively track rest-activity cycles and mobility-related activities, contributing to a better understanding of how these factors impact dementia progression and overall well-being. However, while much attention has been given to physical activity and sleep patterns, relatively few studies focus on social interaction and functioning in dementia patients. This gap is particularly noticeable in research exploring interpersonal physiological synchrony between PWD and their caregivers, an area which we believe can provide novel insights into the health of both PWD and those that care for them. Physiological linkage, which refers to the degree that people's physiological responses change in coordinated ways, can serve as a proxy measure for social connectedness. We hypothesized that decreased physiological linkage during interactions between PWDs and their family caregivers would be associated with diminished ability of PWDs to recognize caregiver emotions.

Experimental Design: In a sample of 28 PWD-family caregiver dyads, we quantified physiological linkage as the positive ("in-phase") correlations between PWD's and caregiver's somatic activity. Somatic activity was measured remotely via actigraphy using wristwatches worn by both partners in their homes during waking hours for 7 days. PWD's cognitive functioning was assessed using Mini Mental Status Exams. PWDs' emotional functioning was quantified as the ability to recognize positive and negative emotions of their caregivers accurately during a 10-minute conflict conversation in our laboratory prior to the 7-day home assessment. Regression analyses (adjusting for PWD's disease severity, assessed using Clinical Dementia Rating Scale) were performed to determine the independent associations between physiological linkage and cognition, recognition of positive emotions, and recognition of negative emotions.

Data and Results: Our analyses revealed that lower physiological linkage between PWDs and caregivers was associated with PWDs' lower emotion recognition of their caregivers' negative emotions (β = .54, p = .02). However, lower physiological linkage was not associated with lower cognitive functioning (β = -.31, p = .15) or recognition of caregiver's positive emotions (β = .10, p = .65).

Conclusion: These results support the hypothesis that diminished physiological linkage is associated with greater impairment of emotional recognition in PWDs. This suggests that impaired emotional recognition contributes to decreased social connectedness in a manner independent from overall cognitive function. Establishing a relationship between PWDs' deficits in emotional awareness and diminished physiological linkage during conversations with their caregivers provides a basis for understanding problems in establishing social connections that are often observed in PWDs, which may be useful in guiding the development of targeted behavioral and psychotherapy for patients with dementia. Further inquiry into the underexplored relationship between physiological synchronicity, social interactions and the overall health of PWD and their caregivers may hold reveal additional insights to improve our understanding and care of those affected by dementia.

DUAL MONTAGE HIGH-DEFINITION TRANSCRANIAL DIRECT CURRENT STIMULATION (HD-TDCS) MODULATES THE NEURAL DYNAMICS SERVING WORKING MEMORY

Peihan J. Huang[1,2], Jake J. Son[1,3], Yasra Arif[1], Jason A. John[1], Nathan M. Petro[1], Maggie P. Rempe[1,3], Kellen M. McDonald[1,2], Lauren K. Webert[1], Grant M. Garrison[1], Hannah J. Okelberry[1], Kennedy A. Kress[1], Tony W. Wilson[1,2,3]

[1] Institute for Human Neuroscience, Boys Town National Research Hospital, Omaha, NE, USA
[2] Department of Pharmacology & Neuroscience, Creighton University, Omaha, NE, USA
[3] College of Medicine, University of Nebraska Medical Center (UNMC), Omaha, NE, USA

Background: Verbal working memory is a critical cognitive construct that supports a variety of daily activities, including social interactions, planning, and abstract reasoning. Neuroimaging studies have highlighted the involvement of prefrontal-occipital circuitry supporting working memory (WM) processes, but the contribution of these regions to overall network processing and possible laterality effects remain poorly understood. Transcranial direct current stimulation (tDCS) is an emerging technique that noninvasively modulates the excitability of neural populations by applying weak electric fields to the scalp. Recent work has shown that such stimulation affects both local cortices and those distant but connected to the site of stimulation. Herein, we evaluate the impact of a novel dual-montage, high-definition tDCS (HD-tDCS) approach on the neural processes serving WM function in healthy adults.

Hypothesis: Stimulation of the left prefrontal-midline occipital regions in parallel will elicit unique alterations in the neural oscillations serving verbal WM processing compared to sham and right prefrontal-midline occipital stimulation, while other critical neural regions for verbal WM processing will be altered by both left- and right prefrontal-midline occipital stimulation relative to sham.

Experimental Design: We utilized dual montage HD-tDCS with 2.0 mA anodal stimulation applied over the midline occipital cortices and either the left or right dorsolateral prefrontal cortices (DLPFC). Our randomized crossover design included 50 healthy adults that received HD-tDCS (left DLPFC-midline occipital, right DLPFC-midline occipital, and sham) during three separate sessions approximately one week apart. Following 20 minutes of stimulation, participants completed a verbal WM task during magnetoencephalography (MEG). All MEG data were imaged separately per stimulation condition using a beamforming approach, and the resulting maps were subjected to voxel-wise 1 × 3 repeated measure ANOVAs to probe stimulation effects.

Results: During the encoding phase of WM processing, left DLPFC-occipital stimulation induced stronger theta responses in the left superior temporal cortices relative to both right DLPFC-occipital stimulation and sham. Additionally, stronger theta oscillations were found in the left precuneus, left inferior parietal, and right parietal cortices following both left DLPFC-occipital and right DLPFC-occipital stimulation compared to sham. Interestingly, attenuated alpha oscillatory responses were found in the right inferior frontal cortices and the right cerebellum following both left DLPFC-occipital and right DLPFC-occipital stimulation relative to sham. Finally, modulatory effects on weaker alpha responses in the bilateral parietal cortices were found following right DLPFC-occipital compared to left DLPFC-occipital stimulation and sham. During the maintenance phase, weaker alpha responses in the left inferior frontal cortices and stronger gamma oscillations in the right occipital cortices were observed following both left DLPFC-occipital and right DLPFC-occipital stimulation relative to sham.

Conclusion: Our results suggest that dual montage anodal HD-tDCS differentially modulates spectrally- and temporally-distinct oscillatory responses within the brain regions supporting verbal WM function. Overall, these findings support the notion that left and right prefrontal regions, and interconnected regions of the cortex, may contribute differently to WM processing, and that tDCS holds promise in distinguishing the unique contribution of each region in the network.

NEUROPILIN-2 (NRP2) IS ASSOCIATED WITH IMMUNE MILIEU OF PANCREATIC DUCTAL ADENOCARCINOMA

Esther Johnson, Sophia Kisling, Zahraa Wajih Alsafwani, Ashu Shah, Surinder K Batra.
Department of Biochemistry & Molecular Biology, University of Nebraska Medical Center, Omaha, NE.

Background and Significance: Among the cancers that contribute to mortality, pancreatic ductal adenocarcinoma (PDAC) shows up as the third leading cause of cancer death in both sexes combined. PDAC is characterized by early-stage metastasis, desmoplastic stroma, and immune suppressive milieu. Neuropilin-2 (NRP2), an axonal guidance molecule, is associated with cancer progression and metastasis by involving lymphangiogenesis, immune tolerance, and angiogenesis. NRP2 levels increase with the differentiation of monocytes to dendritic cells and macrophages, the latter of which is involved in tumor progression. The current study focused on determining NRP2 expression on different cell subsets in PDAC tumors.

Hypothesis: NRP2 expression is linked with immune regulation in PDAC patients.

Experimental Design/Methods: We performed an expression analysis of NRP2 in publicly available bulk RNA and scRNAseq datasets. The expression was validated in PDAC and KPC tumors using immunohistochemistry (IHC) experiments. Flow cytometry and IHC experiments were performed to analyze the population of immune cells expressing NRP2.

Results: TCGA analysis showed a higher expression of NRP2 (~4.5-fold) in the human PDAC tissues (n=179) than normal adjacent control samples (n=171) and a strong association with poorer overall survival (p= 0.017) of PDAC patients. PDAC patients with advanced disease had higher NRP2 expression than early-stage cases. Similarly, in KPC (KrasG12D; Trp53R172H; Pdx-1cre) mice that recapitulate human PDAC disease, NRP2 expression increased in age-wise manner from 5wk to 25 weeks. The cell-specific expression analysis of NRP2 in the publicly available scRNAseq dataset (PAAD_CRA001160) suggested its distinct expression in cancer cells, fibroblasts, endothelial cells, and a specific population of T cells (CD8Tex). Cibersort TIMER analysis suggested a strong correlation of NRP2 with $CD8^+$ T cells (p=7.69e-09) and Treg cells (p= 2.04e-03) in TCGA data of PDAC patients. Flow cytometry analysis on the spleen of KPC mice (25 weeks) indicated a higher expression of NRP2 on $CD8^+$ T cells and regulatory T (Treg) cells indicating its association with immune function regulation in PDAC.

Conclusions and Future Perspectives: Higher expression of NRP2 is associated with poor survival of PDAC patients and it is highly expressed on CD8+ T cells and Treg cells.

ERK 1/2 INHIBITION DECREASES THE NUMBER OF INFILTRATING IMMUNE CELLS IN THE COCHLEA FOLLOWING NOISE EXPOSURE AND PROTECTS FROM HEARING LOSS

Anjali Joseph, Richard Lutze, Matthew Ingersoll, Alena Thotam, Tal Teitz (Creighton University School of Medicine, Omaha, NE)

Background, Significance, Hypothesis

Hearing loss is a widespread disability, but no FDA approved treatments currently exist for the treatment of noise induced hearing loss (NIHL). Therefore, there is a clinical need to develop compounds that can protect individuals from this very common disorder. The mitogen activated protein kinase (MAPK) pathway is commonly deregulated in various types of cancer. Though the MAPK pathway has traditionally been associated with cell proliferation and survival, studies have shown that the MAPK pathway also affects inflammatory signaling and immune responses. In the current literature, inflammation and the innate immune response are shown to be increased by noise exposure, and our lab has previously shown that the MAPK pathway is activated after noise exposure.

Tizaterkib is an anticancer drug currently in phase 1 clinical trials which inhibits ERK1/2, the main kinase in the MAPK pathway phosphorylation cascade. Inhibition of the MAPK pathway by tizaterkib and other MAPK inhibitors provides protection against NIHL in mice. In this study, we aim to find a possible mechanism by which MAPK inhibition protects against NIHL. We hypothesize that tizaterkib administration after noise exposure reduces immune cell infiltration in the inner ear.

Methods

Mice were divided into four treatment groups: carrier alone, tizaterkib alone, noise alone, and noise plus tizaterkib. Mice which were exposed to noise received 100 dB for 2 hours at 8-16 kHz octave band, and those which were treated received carrier or 0.5 mg/kg tizaterkib for three days, twice a day. Mice were then sacrificed 1 hour after the last drug treatment and their cochleae were harvested. Samples were cryosectioned and stained with an anti-CD45 antibody and DAPI to determine the number of total immune cells in the cochlea following noise insult. Samples were imaged using the Zeiss 700 upright confocal microscope and analyzed using the Imaris cell imaging software.

Results

Imaging the total cochleae revealed that four days after noise exposure, mice in the noise-exposed only group had an average of 34±5 CD45-positive cells per section, while noise-exposed mice treated with Tizaterkib had an average of 19±2 CD45+ cells per section. This difference was particularly pronounced in the scala tympani region, indicating that immune cells are concentrating here after noise exposure.

Conclusion

Tizaterkib administration decreased the number of CD45+ cells in the scala tympani, stria vascularis, and total mouse cochlea post noise exposure, suggesting that the protective effect of tizaterkib is partially due to a reduction in immune cell infiltration of the cochlea. This supports the hypothesis that immune cell infiltration, shown by other literature to be 95% macrophages, is a contributing factor to hearing loss following damaging noise insults.

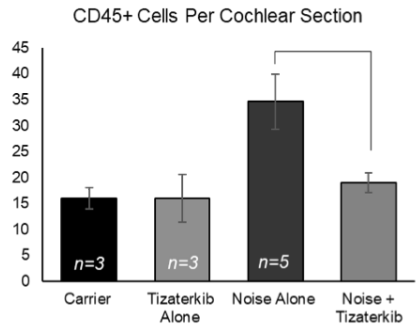

Figure 1: Tizaterkib treatment lowers the number of CD45 positive cells in the cochlea 4 days' post noise exposure.

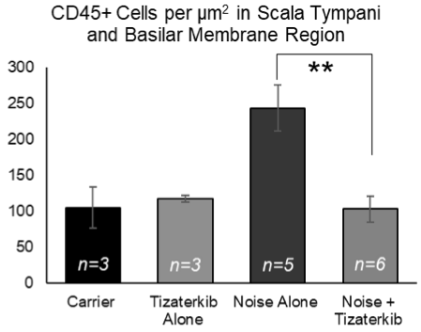

Figure 2: Tizaterkib treatment lowers the number of CD45 positive cells in the walls of the scala tympani 4 days' post noise exposure

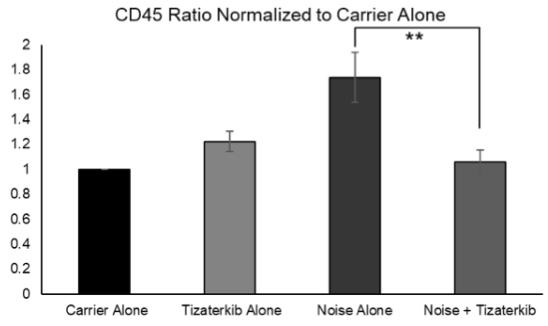

Figure 3: Tizaterkib treatment lowers the amount of CD45 and CD68 in the cochlea 6 days' post noise exposure.

NEOADJUVANT GENE THERAPY WITH CALRETICULIN AND R848: A NOVEL APPROACH TO PANCREATIC CANCER TREATMENT.

Ekta Kapoor, Farhana Islam, David Vetvicka, David Oupický
University of Nebraska Medical Center, Omaha, Nebraska

Background, Significance, and Hypothesis: Pancreatic ductal adenocarcinoma (PDAC) is an aggressive malignancy with a 5-year survival rate of 13%, accounting for an estimated 51,750 deaths in 2024 in the United States. Limited treatment options for advanced PDAC necessitate innovative therapeutic strategies. Immunotherapy offers a promising alternative, with immunogenic cell death (ICD) emerging as a potential anti-tumor mechanism. ICD is characterized by the exposure of calreticulin (CALR) as ecto-CALR on dying cells, acting as an “eat me” signal to dendritic cells (DCs). This triggers phagocytosis, DC activation, and subsequent T-cell-mediated immune responses.
In this study, an engineered mRNA encoding CALR fused with the Daf-1 gene sequence was developed (mCALR-Daf1), enabling glycosylphosphatidylinositol (GPI)-anchoring of CALR on tumor cell membranes. The mRNA was encapsulated in an in-house formulated lipid nanoparticle (LNP) (called FI-3) delivery system to ensure efficient delivery to PDAC tumors when administered intraperitoneally (I.P). The treatment was combined with R848 (Resiquimod), a Toll-like receptor 7/8 agonist, to enhance antigen-presenting cell (APC) recruitment and activation.
This combination therapy was hypothesized to synergistically boost ICD, augment anti-tumor immune responses, and reduce recurrence risks in PDAC. Preliminary findings indicate this approach holds potential as a novel therapeutic modality, paving the way for improved PDAC management. Further preclinical studies are underway to validate these findings and optimize treatment protocols.

Experimental Design: This study employed both in vitro and in vivo approaches to evaluate the therapeutic potential of the engineered FI-3 lipid nanoparticle (LNP) loaded with mCALR-Daf1 administered in combination with the TLR7/8 agonist R848 for pancreatic ductal adenocarcinoma (PDAC).
In vitro studies: FI-3 was characterized for size, encapsulation efficiency, and stability over 15 days in PBS at 4°C using dynamic light scattering (DLS) and the RiboGreen assay. The transfection efficiency of FI-3/mCALR-Daf1 was assessed using Lipofectamine MessengerMAX as a benchmark. Biodistribution studies confirmed FI-3 delivery to PDAC tumors after I.P. administration in mice.
In vivo studies: Male C57/BL6 mice were orthotopically implanted with KPC8060 PDAC cells and divided into three groups: Group 1 (Untreated control), Group 2 (R848-treated), and Group 3 (Combination therapy with FI-3/mCALR-Daf1 and R848). Therapeutic efficacy was assessed by comparing tumor weights across groups. Immune profiling of tumors, using multi-color flow cytometry, was performed to evaluate the modulation of immune cell populations in the tumor microenvironment. Other analyses included apoptosis using TUNEL assays, immunohistochemistry, and cytokine profiling to investigate immune activation and cell death mechanisms.
This design aimed to elucidate the combined therapy's ability to induce immunogenic cell death, enhance immune response, and reduce tumor burden, providing insights into its potential as an effective PDAC treatment.

Results/ Data:

Table 1: Summary of the physico-chemical properties of FI-3

Day	Encapsulation efficiency %	Particle size (d. nm)	PDI
Day 0	98.1	65.91	0.18
Day 1	97.7	66.67	0.18
Day 7	96.5	71.10	0.22
Day 10	98.1	75.50	0.22
Day 14	98.1	76.69	0.26

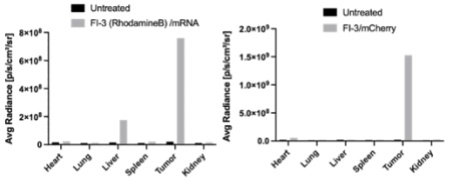

Fig 2: Biodistribution of Rhodamine B-labeled FI-3/mRNA in KPC8060 orthotropic PDAC mice through IP administration (A) *Ex vivo* Rhodamine B fluorescence images of the tumor and major organs at 12 h after injection. Rhodamine B (Ex=546 nm, Em=567 nm). (B) Quantification of Rhodamine B fluorescence intensity in tumor and different organs at 12 h.

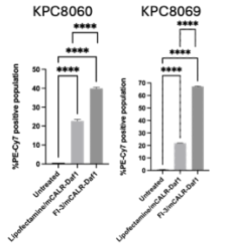

Fig1: FACS analysis of transfection efficiency of FI-3 LNP vs Lipofectamine MessengerMAX in KPC8069. Calreticulin expression in A) KPC8060 and B) KPC8069 untreated and transfected with Lipofectamine/mCALR-Daf1 vs LNP FI-3/mCALR-Daf1. Data are depicted as mean ± SEM (n=3), with individual data points shown. Comparisons are unpaired t-tests between all the groups after 48 hours of treatment. *P < 0.05; **P < 0.01; ***P < 0.001; ****P < 0.0001

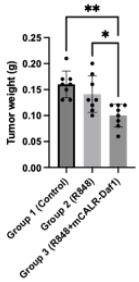

Fig 3: Tumor weight. Tumor mass in cell lines KPC8060 implanted orthotopically (OT), allocated to the vehicle (V), or R848, or combination (R848 + mCALR-Daf1) treatment groups. Comparisons are ordinary one-way ANOVA analyzing groups, with multiple comparison analyses after treatment. *P < 0.01; **P < 0.05; ***P < 0.01; ****P < 0.001

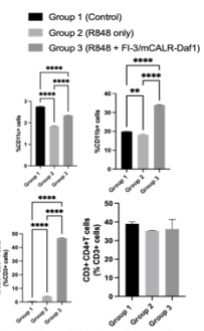

Fig 4: Effect of R848 vs. R848 + FI-3/mCALR-Daf1 on tumor immune microenvironment. Data are depicted as mean ± SEM (n = 8/group). Comparisons are two-way ANOVA analyzing groups, with multiple comparison analyses of the main column effect at the end of treatment. *P < 0.05; **P < 0.01; ***P < 0.001; ****P < 0.0001

Conclusion:

- The lipid nanoparticle (LNP) FI-3 demonstrated excellent stability, with a size of 65–76 nm and ~98% encapsulation efficiency over 15 days at 4°C in PBS.
- FI-3 showed superior transfection efficiency compared to Lipofectamine MessengerMAX.
- Intraperitoneal administration of FI-3 successfully delivered mRNA to PDAC tumors.
- Combination therapy with R848 and FI-3/mCALR-Daf1 significantly reduced tumor weight in PDAC mice.
- The treatment enhanced apoptosis, modulated anti-inflammatory cytokines, and increased anti-tumor immune cell infiltration in the tumor microenvironment.

hFWE IS DECREASED IN POORLY-DIFFERENTIATED CUTANEOUS SQUAMOUS CELL CARCINOMA TUMORS AND INDUCED BY UV IRRADIATION IN KERATINOCYTES

Patrick T. Kuwong[1], Justin C. Rudd[1], Megan Vo[1], James A. Grunkemeyer[1], Andrew Siref[2], Shuai Li[2], Poonam Sharma[2], Laura A. Hansen[1]
[1]Creighton University School of Medicine, Department of Biomedical Sciences, Omaha NE.
[2]Department of Pathology, Creighton University School of Medicine, Omaha, NE

BACKGROUND: UV-induced damage in epidermal keratinocytes causes numerous physiological changes that eventually lead to premature skin aging and squamous cell carcinoma (SCC). SCC is the second most common cancer in the US, with an estimated 1 million cases every year. Thus, there is need for improved understanding of the UV-related physiological changes in keratinocytes that lead to the development and progression of SCC. Epidermal keratinocytes, the cells from which cSCCs originate, form skin by organizing into stratified squamous epithelium. These cells stratify into basal, spinous, granular layers, and the topmost cornified layers as they undergo a differentiation program, characterized by a series of physiological and morphological changes.

SIGNIFICANCE: Our lab recently showed that human Flower (hFWE), a putative calcium channel of unknown function in keratinocytes, is increased as keratinocytes differentiate both *in vitro* and *in vivo*. To better understand the role of hFWE in SCC development and progression, we questioned whether **(1)** *hFWE* expression is decreased in poorly-differentiated SCC tumors *in vivo*, and whether **(2)** hFWE expression is induced after UV-induced keratinocyte stress *in vitro*.

HYPOTHESIS: We hypothesized that **(1)** hFWE expression would be increased in well-differentiated compared to poorly-differentiated SCC, and **(2)** that hFWE expression would be induced by UV-induced keratinocyte stress.

EXPERIMENTAL DESIGN: To test our hypotheses, two independent experiments were conducted. First, we evaluated the expression of hFWE in well-differentiated and poorly-differentiated SCC tumors. Immunofluorescence for hFWE (Rabbit polyclonal-1:200) was performed on formalin fixed, paraffin-embedded human SCC tumors (N=5). Automated quantification was performed using Olympus VS-ASW software. And second, the effect of UV-induced stress on hFWE expression was assessed *in vitro*. SCC-13 keratinocytes were exposed to three different doses of UV (0 J/m², 500 J/m², and 1000 J/m²; N=2). Protein was collected from these samples and immunoblotting for hFWE (Rabbit polyclonal-1:1000) and Tubulin (Cell Signaling-1:1000) was performed. Densitometric analysis was conducted using Bio-Rad's ImageLab 6.1 software (Bio-Rad Laboratories, Inc, Hercules, CA). Statistical Analysis. Statistical significance was determined using a two-tailed Student's t-test (p-values<0.05) via GraphPad Prism 10.02 software (GraphPad Software Inc., Boston, MA).

RESULTS: Immunofluorescence quantification showed that hFWE is highly expressed in differentiated compartments of well-differentiated SCCs and undetectable in poorly-differentiated SCCs. Additionally, Immunoblotting quantification also showed a three-fold increase in hFWE expression in SCC-13 keratinocytes after exposure to 1000 J/m^2 compared to the control.

CONCLUSION: Together, these data indicate that hFWE expression is decreased in poorly-differentiated SCC tumors and is induced by UV irradiation in keratinocytes, suggesting that hFWE may play a role in SCC development and progression.

EVOLVING TRENDS IN U.S. OPIOID MORTALITY: DISPARITIES AND IMAPCT OF COVID-19

Benjamin Leiken, Ricky Rana, Vikram Murugan, Taylor Billion, Abubakar Tauseef, Ali Bin Abdul Jabbar (CUSOM Omaha, NE)

Background, Significance, and Hypothesis: The opioid crisis is a public health challenge in the United States, significantly impacting mortality rates. The COVID-19 pandemic put significant strain on the American healthcare system and inhibited routine access to all forms of healthcare, including addiction treatment and rehabilitation services. Epidemiological evidence suggests a disproportionate impact of the opioid crisis across varying regions, ethnicities, races, and socioeconomic groups. We hypothesize that that the opioid crisis has been further exacerbated by the COVID-19 pandemic, contributing to a surge in substance use and overdose deaths.

Experimental Design: Data from the CDC Wonder Database was used to identify opioid use-related deaths in the United States from 1999 to 2023. Crude and age-adjusted mortality rates (AAMR) were calculated across different across different census regions, racial groups, genders, and states. Temporal trends in mortality were analyzed using the Joinpoint Regression Program. Annual percentage change (APC) and average annual percentage change (AAPC) in mortality rates were calculated with 95% Confidence Intervals, and APC trends were considered statistically significant with p-value ≤0.05.

Data and results: Opioid-related mortality surged during the COVID-19 period, with significant regional, racial, and state-level disparities. Gender-specific analyses revealed that males had a higher AAPC from 1999 to 2023 of 10.03 compared to females at 9.82. From 2021 to 2023, no significant APCs were observed for either gender. Among racial groups, American Indians/Alaska Natives had the highest AAPC from 1999 to 2023 at 13.85, while Hispanic or Latino individuals had the lowest increase in AAMR from 3.2 in 1999 to 23.0 in 2023. During the COVID-19 period, the APC for American Indians/Alaska Natives was 14.12, indicating a continued significant increase. Black or African American people had the second highest AAMR over the studied years, rising from 2.1 in 1999 to 47.7 in 2023. Non-Hispanic white people had an AAMR increase from 2.8 in 1999 to 32.5 in 2023. The non-Hispanic white APC was 10.986 from 1999-2021 and subsequently decreased to -1.855 from 2021 to 2023. Asian and Pacific Islanders had the lowest AAMR from 0.3 in 1999 to 4.6 in 2023 with an AAPC of 12.057. Every census region saw an increase in AAMR over time, with the Midwest seeing the most significant increase from 1.41 in 1999 to 29.7 in 2023. The West had the lowest rise AAMR from 5.2 in 1999 to 29.6 in 2023. Hawaii, Texas, and California had the lowest change in AAMR from 1999 to 2019, while Maryland, West Virginia, and Delaware had the highest. From 2019 to 2023, New Jersey had the largest drop in AAMR while West Virginia had the largest increase.

Conclusion: Our study shows that the U.S. opioid crisis has escalated during the COVID-19 period, with significant increases in mortality observed across demographic groups and regions. The Midwest, especially West Virginia, saw the highest mortality rates, while Hawaii experienced the smallest exacerbation. Our study highlights ongoing demographic and regional disparities in opioid-related behaviors and mortality, with certain disadvantaged groups particularly affected since COVID-19. Addressing these disparities is essential to reducing substance use-related mortality effectively.

Autonomic Changes are Delayed Relative to Ventricular Enlargement in Post-Hemorrhagic Hydrocephalus

Robert Lowndes, Grace Lai, Eric S Peeples (Creighton, Omaha, NE)

Background, Significance, Hypothesis: Preterm infants born before 32 weeks of gestation possess a highly vascularized and friable germinal matrix vasculature which can easily rupture, resulting in Intraventricular hemorrhage (IVH), and potentially impair cerebral spinal fluid (CSF) reabsorption and obstruction, resulting in post-hemorrhagic hydrocephalus (PHH). The pressure that results in the brain from enlarged ventricles can cause white matter injuries and seizures, as well as neurocognitive impairment, motor dysfunction, and growth impairment in the future. Currently there is no consensus on when to intervene or how to treat patients with PHH. A recent trial (ELVIS trial) showed that specific ultrasound (US)-based ventricular measurement thresholds paired with early interventions were associated with lower odds of death or neurodevelopmental complications. The local historical method to determine intervention timing relied on symptoms alone, but it is not clear how these symptoms relate to the ventricular measurements. We hypothesized that patients cross the US-based ventricular measurements thresholds prior to developing clinical signs such as autonomic changes.

Experimental Design: A retrospective cohort study of infants born before 32 weeks of gestation with grade 2-4 IVH and admitted to the Children's Nebraska or UNMC neonatal intensive care units. Demographics, autonomic events (e.g. average number of documented bradycardic events for the three days starting at 32 or 36 weeks corrected gestational age), and results from serial US were extracted from the electronic health records. On the US, the ventricular indices and anterior horn widths were measured (Fig. 1). Subjects were stratified to: Group 0: never reached the threshold for CSF diversion, Group 1: surpassed the threshold but never underwent CSF diversion, Group 2: surpassed the threshold and underwent CSF diversion. Categorical variables were analyzed by Fisher's Exact Test and continuous variables were analyzed by the Kruskal-Wallis Test.

Data and Results: The average corrected gestational age at the time of shunting was 32.8 ± 4.4 weeks. Using clinical symptoms alone, infants in Group 2 received a shunt on average ~27 days after crossing the ventricular measurement threshold for CSF Diversion. Most patients crossed the diversion threshold by 28 weeks, but a few crossed as late as 31 weeks (Fig. 2). Group 1 had more bradycardic events (mean 5.3 vs. 4.0/day) at 36 weeks corrected but smaller head circumference (mean 28.2 vs. 29.8 cm) at 32 weeks corrected vs. Group 2. Four infants who would have met US guidelines for diversion never underwent surgical intervention.

Conclusion: Infants in this cohort met US-based thresholds nearly 4 weeks prior to having severe enough clinical symptoms to drive surgical intervention. The patients that crossed the threshold later displays the importance of frequent US screenings up to 31-32 weeks. Future studies should assess the potential neurodevelopmental impacts of this management.

Figure 1. Anterior horn width (AHW) and ventricular index (VI) measures

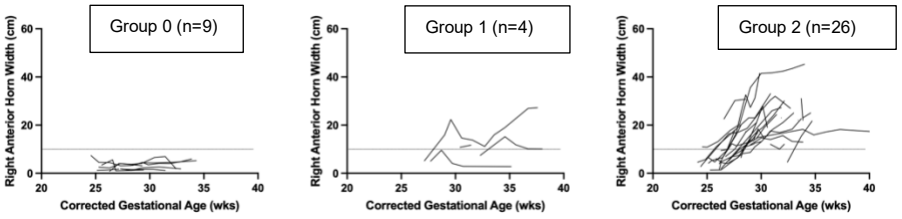

Figure 2. Anterior horn widths (AHW) over time, stratified by group, with the published threshold of 10 cm (based on El Dib et al) shown by a dotted line

DECIPHERING A NOVEL MECHANISM FOR CIGARETTE SMOKE-INDUCED INITIATION OF PANCREATIC CANCER

Poompozhil Mathivanan[1], Pratima Raut[1], and Moorthy P. Ponnusamy[1&2] and Surinder K. Batra[1&2].

[1]Department of Biochemistry and Molecular Biology, University of Nebraska Medical Center, Omaha, NE.

Background and Significance: Cancer is the second leading cause of death in the United States (US), accounting for approximately 611,720 deaths in 2024, or around 1,680 deaths per day. Among these, 30% (around 183,516 deaths) are primarily attributed to cigarette/tobacco smoking and tobacco-related products. Cigarette smoking remains the most preventable cause of cancer-related deaths in the US. Currently, about 29 million adults (12% of the population) are diagnosed as current smokers and these individuals have an increased risk of developing at least 12 different types of cancer, including pancreatic cancer. Pancreatic cancer is a lethal cancer having a 5-year survival rate of only 13%. Smokers have twice the risk of developing pancreatic cancer and experience a worse prognosis when diagnosed compared to non-smokers. In this study, we aim to explore the mechanism by which cigarette smoking and other tobacco products contribute to the initiation of pancreatic cancer and to target the genes that are upregulated in smokers alone. An understanding of how cigarette smoke causes the development of pancreatic cancer could help reduce the incidence of not only pancreatic cancer but also other tobacco-related cancers.

Hypothesis: Gpr15 overexpressed in pancreatic ductal adenocarcinoma (PDAC) patients with a history of smoking may contribute to tumor progression and thus targeting it can be a novel therapeutic outcome in PDAC patients.

Experimental Design/Methods: Differentially expressed genes (DEGs) were validated using publicly available datasets comparing current smokers and lifelong non-smokers in pancreatic and lung cancers. The top-upregulated gene was further validated *in vitro* using western blot, qPCR, and immunofluorescence in human normal pancreatic cells (HPNE) and pancreatic cancer cells (CD18/HPAFII). These cells were treated with commercially available cigarette smoke extract (CSE) for 24 hours, 48 hours, and 10 days. The CSE (40 mg/ml condensate) was prepared by smoking the University of Kentucky 3R4F Standard Research Cigarettes. Subsequently, the HPNE and CD18 cells were exposed to carcinogenic and non-carcinogenic chemicals found in cigarette smoke, such as nicotine, NNN, and NNK, for 10-days. Functional assays were performed on the 10-day-treated cells to assess proliferation rates using Incucyte and colony-forming ability. A stable knockdown model of HPNE and CD18/HPAFII cells using shRNA was developed and subjected to functional assays. *In vivo* validation was carried out using immunohistochemistry on tissue samples from K-rasLSL.G12D/+; Pdx-1-Cre (KC) mice exposed to cigarette smoke for 20 weeks.

Results: Among the differentially expressed genes, G-protein coupled receptor 15 (Gpr15) was identified as the most significantly upregulated gene. Western blot and qPCR analyses revealed increased Gpr15 expression in cells treated with cigarette smoke extract, compared to controls of the same duration. Gpr15 expression was found to increase in proportion to the duration of treatment with CSE. Cells treated with NNK exhibited the highest expression of Gpr15 in comparison to those treated with NNN or nicotine. Treatment cells of 10 days duration showed enhanced proliferation rates compared to control cells, thus inferring that cigarette smoke increased the proliferation ability of the cells. However, Gpr15 knockdown cells even after being treated with CSE for 5 days exhibited a reduced proliferation rate. In vivo, validation using KC mouse models revealed increased Gpr15 expression in smoke-exposed tissues compared to controls.

Conclusions and Future Perspectives: Our results demonstrate that Gpr15 expression is increased in proportion to the treatment with commercially available cigarette smoke extract. Our futuristic goals are to unravel the mechanism by which cigarette smoke enhances Gpr15 expression and to decipher the role of Gpr15 in the initiation of pancreatic cancer.

IMPACT OF MATERNAL RACE AND ETHNICITY ON EXCLUSIVE BREASTFEEDING IN A NORMAL NEWBORN NURSERY

Emily May, Gena Fuller, Terence Zach (Creighton University School of Medicine Omaha, NE)

Background and Significance: Exclusive breastfeeding (EBF) for the first six months is recommended by leading health organizations for its significant benefits to maternal and infant health. However, national data highlights disparities in breastfeeding rates across racial and ethnic groups. This study aims to examine the relationship between maternal race/ethnicity and EBF rates among infants in a normal newborn nursery.

Methods: Data were retrospectively collected from 253 infants admitted to the Creighton University Medical Center–Bergan Mercy Hospital mother-baby unit in August 2023. Maternal race and ethnicity were recorded, and feeding practices were categorized as EBF or formula-fed. Mothers who did not specify race (n=38) or ethnicity (n=19) were excluded. Statistical analysis included chi-squared tests with two-tailed p-values.

Results: Hispanic mothers were significantly less likely to EBF compared to non-Hispanic mothers (p=0.0002). When stratified by race, the trend persisted (p=0.01). No significant differences in EBF were observed among racial groups (p=0.69). Small sample sizes for specific groups, such as American Indian/Alaska Native, Native Hawaiian, and Asian mothers, may have limited the power to detect racial differences.

Conclusions: Hispanic mothers demonstrated lower EBF rates, consistent with national trends of higher formula supplementation within 48 hours postpartum. Cultural perceptions, economic pressures, and early return to work may contribute to this disparity. Future research should explore socioeconomic determinants, including education, employment type, income, and healthcare access, to better understand and address barriers to EBF across all racial and ethnic groups.

ASSESSING THE EFFECTIVENESS AND STUDENT PERCEPTIONS OF A TWO-WEEK ANESTHESIOLOGY ELECTIVE ROTATION FOR THIRD YEAR MEDICAL STUDENTS

Joel R. Meyers, Ashley L. Rensted, Alexander G. Hall, Mark D. Reisbig, (Creighton University Omaha, NE)

Background, Significance, Hypothesis: Anesthesiology is a quickly growing field: 1,681 US MD seniors applied into the specialty in 2024, compared to 1,162 in 2014.[1-2] Creighton University School of Medicine does not currently have a residency program but hopes to expose third-year medical students to the specialty by offering a two-week anesthesia elective course. Because most US medical schools teach the pre-clinical years by organ system, anesthesia does not get the same representation in the curricula that other specialties may receive.[3] This study aims to look at the impact that a two-week anesthesiology elective had on third-year medical students' perceived knowledge about the specialty as well as the overall effectiveness of the elective.

Experimental Design: We designed a survey to assess respondents' perceived understanding of various elements of anesthesiology and their comfort level with different procedures. Responses to these questions were assessed both before and after completing the two-week elective with a four-point Likert scale. The survey was distributed to all third-year medical students enrolled in the elective from 12/2022 to 9/2024. 34 responses were included in the analysis after removing responses that did not fill out both the pre and post-elective surveys or didn't provide their student ID to link responses. Paired t-tests were used to compare the differences in ratings.

Data and Results: There was a significant increase from pre-elective to post-elective in self-reported level of understanding across all 10 areas surveyed, which represented various elements of anesthesiology (Table 1). There is also a significant increase in self-reported level of comfort with skills except for epidural or spinal anesthesia and placing an arterial line or a central line (Table 2).

Conclusion: This two-week, optional third-year anesthesiology elective is effective at increasing students' self-perceived knowledge of the basic responsibilities and skills of an anesthesiologist. However, this elective does not significantly influence students' intention to pursue a career in anesthesiology. Based on the responses to the short answer questions, some areas for improvement include adding more 1:1 time for students with the anesthesiologists and adding more structure to the elective with additional lectures to cover pertinent topics such as ventilator settings and pharmacology.

Table 1: Change in Self-Reported Level of Understanding. Students reported a significant increase in their perceived understanding of various aspects of the specialty. Understanding was ranked on a scale from 1 (very poor) to 4 (very good).

N=34	Pre Mean (sd)	Post Mean (sd)	95% CI of Difference	*P*
What an anesthesiologist does from day to day	2.56 (0.56)	2.94 (0.55)	(0.12, 0.64)	.005
The interpersonal/ communication skills needed to be an anesthesiologist	2.62 (0.55)	3.21 (0.48)	(0.34, 0.83)	<.001
Non-technical skills required…	2.68 (0.59)	3.12 (0.48)	(0.21, 0.67)	<.001
Role of anesthesiologist vs CRNA	2.18 (0.80)	3.06 (0.65)	(0.53, 1.23)	<.001
The various subspecialties of anesthesiology available	1.97 (0.76)	2.71 (0.83)	(0.43, 1.04)	<.001
What is assessed during a pre-op anesthesia evaluation	2.29 (0.80)	3.09 (0.71)	(0.49, 1.10)	<.001
Factors that contribute to difficult intubation or poor response to anesthesia	2.35 (0.69)	3.21 (0.69)	(0.50 1.21)	<.001
Basics of general anesthetics and their side effects	2.18 (0.63)	2.88 (0.69)	(0.44, 0.97)	<.001
Multimodal pain management	2.18 (0.72)	2.68 (0.68)	(0.23, 0.78)	<.001
Ventilator settings	1.88 (0.88)	2.44 (0.79)	(0.24, 0.88)	.001

Table 2: Change in Self-Reported Level of Comfort. Students reported a significant increase in comfort in all areas assessed except for placing an arterial or central line and epidural or spinal anesthesia. Comfort was ranked on a scale from 1 (not at all comfortable) to 4 (very comfortable).

N=34	Pre Mean (sd)	Post Mean (sd)	95% CI of Difference	*P*
Endotracheal tube placement	1.59 (0.61)	2.32 (0.77)	(0.41, 1.06)	<.001
Mask ventilation	2.24 (0.89)	2.97 (0.80)	(0.31, 1.16)	.001
Starting an IV	1.71 (0.91)	2.47 (0.79)	(0.39, 1.14)	<.001
Reading a vitals monitor	2.62 (0.95)	3.18 (0.67)	(0.29, 0.83)	<.001
Placing an arterial line or a central line	1.18 (0.46)	1.24 (0.50)	(-0.15, 0.27)	.571
Medication administration and dosing	1.41 (0.61)	1.82 (0.80)	(0.15, 0.67)	.003
Epidural or spinal anesthesia	1.29 (0.46)	1.47 (0.66)	(-0.07, 0.43)	.160

ENHANCING LEARNING OUTCOMES IN ELECTROCARDIOGRAM INTERPRETATION: A QUALITY IMPROVEMENT INITIATIVE USING AN ONLINE INTERACTIVE TOOL

Dominick Milkie, Issa Asfour, MD; Attila Roka, MD, PhD (Creighton University School of Medicine, Omaha, Nebraska)

Background: Electrocardiogram (ECG) interpretation is a core competency for cardiology fellows education, yet clinical training rotations often provide insufficient exposure to complex ECG cases, limiting the development of diagnostic proficiency. To address this challenge, ECGschool.com was developed by Attila Roka MD, PhD and Issa Asfour MD as an online platform offering 100 challenging ECG cases across 25 key interpretation areas. The platform aims to improve ECG interpretation skills, diagnostic accuracy, and confidence among cardiology fellows through automated feedback and performance tracking.

Significance of Problem: Insufficient ECG interpretation training can compromise patient care, as accurate interpretation is essential for diagnosing and managing potentially life-threatening cardiovascular conditions. Addressing this educational shortfall through innovative learning tools is essential to ensure fellows achieve the proficiency needed for high-quality patient care and to bridge the gaps left by traditional clinical training.

Hypothesis, Problem, or Question: Does the use of an online platform like ECGschool.com improve ECG interpretation skills, confidence, and diagnostic accuracy among cardiology fellows, and can it effectively address the educational gaps in traditional clinical training?

Experimental Design: A cohort of 20 cardiology fellows participated in this quality improvement initiative. Participants engaged in unsupervised practice sessions using ECGschool.com. The platform recorded metrics including response times, accuracy rates, and progression in proficiency across the 25 interpretation areas. Pre- and post-practice surveys evaluated fellows' confidence and satisfaction levels, while de-identified data analysis assessed the educational impact. The initiative also incorporated a comparative analysis of pre-and post-practice diagnostic accuracy to quantify improvement.

Results/Data: Participants completed an average of 53 out of 100 ECG cases, with a mean response time of 229 seconds per case. The strongest areas of performance were QRS morphology (100% accuracy), ventricular arrhythmias (90% accuracy), and ischemia/injury interpretation (88% accuracy). The weakest areas included regularity (69% accuracy) and pacemaker interpretation (70% accuracy). Survey feedback revealed that 80% of participants perceived an improvement in their ECG interpretation accuracy, 60% found the cases challenging, and 100% reported the feedback as helpful in identifying areas for improvement.

Conclusions: ECGschool.com significantly improved fellows' confidence and accuracy in interpreting complex ECGs, with notable proficiency in areas such as QRS morphology and ventricular arrhythmias. However, weaker areas, including regularity and pacemaker interpretation, highlight opportunities for further development. Future directions include expanding the platform to medical students and residents with stratified curricula tailored to experience levels. Planned enhancements, such as adaptive learning, leaderboards, milestones, and badges, aim to increase engagement and optimize learning outcomes. This initiative demonstrates the potential of technology-driven education to address gaps in clinical training, ultimately contributing to improved patient care.

EFFECTS OF PUBERTY ON ANTERIOR PITUITARY VOLUME AND SYMPTOMOLOGY IN ADOLESCENTS WITH AUTISM SPECTRUM DISORDER: A PILOT STUDY

Caitlin Mills, Holly AF Stessman, and Giorgia Picci (CUSOM Omaha, NE)

Background, Significance, Hypothesis: Pubertal effects on brain development in autism spectrum disorders (ASD) are poorly understood, despite documented increases in ASD symptom severity during adolescence for some. Notably, puberty is a time of increased vulnerability for developing psychopathology symptoms for typically developing (TD) and autistic youth alike. A primary brain region responsible for pubertal hormone production is the anterior lobe of the pituitary gland (PG), which exhibits puberty-related increases in size in TD youth. In TD youth, elevated mental health symptoms during adolescence have been linked to a larger PG, suggesting that the PG may be a litmus for puberty-related brain changes and concomitant psychopathology. These processes have never been explored in ASD, which is the current focus of this pilot study. Specifically, this study investigated whether puberty differentially affects anterior pituitary volume in adolescents with ASD and TD, and whether these factors predict symptom severity in ASD.

Experimental Design: Fifty adolescents with ASD and 50 TD controls, ages 9-11 years old, participating in the Adolescent Brain Cognitive Development (ABCD) Study with a T1-weighted MRI scan, pubertal development scales, and autism symptom questionnaires were included. Participants were carefully matched on age, sex, race, ethnicity, socioeconomic status, study site, and pubertal development based on the pubertal development scale. Anterior and posterior lobes of the pituitary gland were manually traced using state-of-the-art methods.

Data and Results: ANCOVA analyses showed that ASD and TD have similar associations in puberty-related increases in anterior, but *not* posterior, pituitary gland volume, although TD youth exhibit a stronger link. In addition, adolescents with ASD in later stages of puberty show trending links between a larger anterior pituitary gland volume and more severe autism symptoms (Figure 2a, b).

Conclusion: These results expand on existing literature showing that some autistic adolescents experience deterioration in function during puberty, by providing a potential neural mechanism that may explain individual differences in this population.

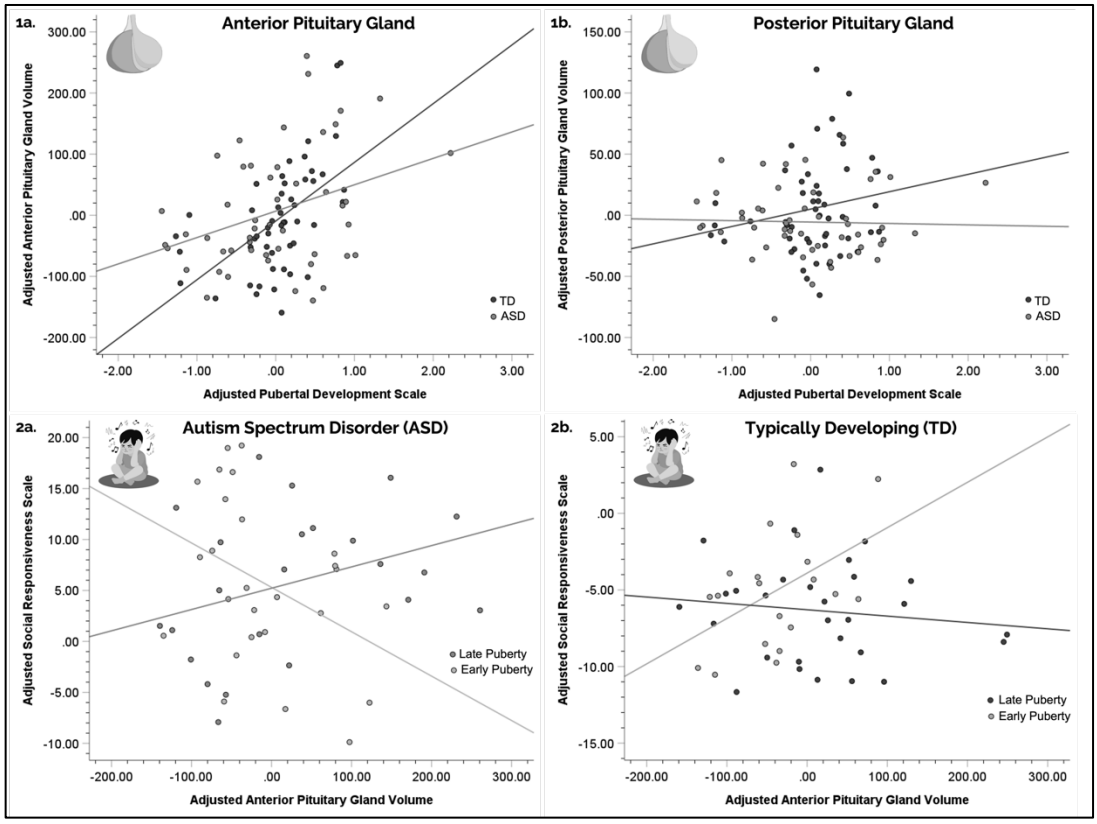

Figure 1a,b: ANCOVA results with a significant group by PDS interaction predicting anterior (a) (p = .02*), but not posterior (b) (p = .15) PG volumes.

Figure 2a,b: ANCOVA results with a significant group by PDS by anterior PG volume interaction predicting social responsiveness scale in ASD (a) and TD (b) (p = .04*). Notably, ASD in later stages of puberty show trending links between a larger anterior PG and more severe autism symptoms (p = .052). The model(s) included age, sex, and total intercranial volume.

IDENTIFYING THE IMPACT OF AGE AND BIOLOGICAL SEX DIFFERENCES IN INVASIVE TREATMENT OF NSTEMI IN PATIENTS WITH DIABETES MELLITUS

Anna Park, Danielle Dilsaver, Michael Del Core (Creighton University School of Medicine Omaha, NE)

Background, Significance, Hypothesis: Diabetes mellitus (DM) is a leading healthcare concern in the United States, with a projected 1 in 3 individuals developing the disease in their lifetime. Among those with diabetes, more than half die as a direct result of cardiovascular disease (CVD). Of the various complications of CVD, myocardial infarctions (MI) are one of the leading causes of hospitalization and morbidity. Non-ST-elevation myocardial infarctions (NSTEMI) are the most common type of MI. Currently, there are two main pathways of treatment for patients with NSTEMI: 1) invasive surgical procedure or 2) non-invasive medical therapy. The traditional treatment for NSTEMI is an invasive surgical procedure, a percutaneous intervention (PCI). PCI involves threading a small catheter through a blood vessel to visualize and subsequently eliminate the blockage in the cardiac artery causing the NSTEMI. Amongst patients with DM, there have been well documented differences in disease course and presentation between biological males and females. Additionally, studies have shown that a patient's age at the time of the NSTEMI event impacts their mortality rate, with an increased age associated with an increased mortality rate. Although previous studies have shown PCI to generally be more effective at decreasing mortality in diabetic patients, it is still unknown how the interplay between individual factors such as biological sex and age impact survival and post-procedural complications in cases of PCI treated NSTEMIs. The aim of this study was to assess post-operative complications and mortality rates in patients treated with PCI for NSTEMI. Additionally, we assessed how DM moderated the effect of age and sex on postoperative complications and mortality.

Experimental Design: Data were abstracted from the National Cardiovascular Data Registry from March 2018 through December 2023. Patients that underwent a PCI for NSTEMI were included in the analysis. Patients were further stratified by DM diagnosis. The primary aim was to assess the difference in adverse events between patients with and without DM. An adverse event was defined as in-hospital death or complication. Complications included MI, cardiogenic shock, heart failure, stroke, cardiac tamponade, vascular complications, and bleeding. The rate of adverse events was stratified by DM diagnosis and compared using a chi-square test or Fisher's exact test, depending on cell counts. To assess whether age and biological sex moderated the effect of diabetes on adverse events, separate log-binomial models were estimated with diabetes-by-age and diabetes-by-biological sex interactions, respectively.

Data and Results: The results showed that mortality did not differ by diabetes status (DM: 2.72% vs non-DM: 1.18%, $p = 0.340$). Diabetes did not moderate the effect of age on risk of death (0.097). Notably, age was significantly associated with risk of inpatient mortality ($p = 0.002$). Post-operative complication rates also did not differ by diabetes status (DM: 1.99% vs non-DM: 3.25%, $p = 0.106$). Within the post-operative complications of cardiogenic shock, heart failure, stroke, cardiac tamponade, and vascular complications, the post-operative rates did not differ by diabetes status (Table 1). However, the rates of the post-operative complications of myocardial infarction and bleeding did differ by diabetes status (Table 1). Diabetes did not moderate the effect of age on risk of post-operative complications (interaction $p = 0.403$). However, age was significantly associated with a risk of post-operative complications ($p < 0.001$). When comparing the effects of diabetes and biological sex on post-operative mortality, we found that the main effect of diabetes alone ($p = 0.566$) and biological sex alone ($p = 0.067$) were not statistically associated with post-operative mortality. Further, DM had did not impact the effect of biological sex on post-operative mortality rates (interaction $p = 0.952$). The main effect of sex did show a significant impact on the rates of post-operative adverse events ($p < 0.001$); females experienced greater rates of both post-operative mortality and complications.

Conclusion: The results showed that the outcomes of mortality rate and post-operative complication rate did not differ by DM status. Additionally, DM did not have a significant moderative effect on the impact of age and biological sex on complications and post-operative mortality in patients being treated with PCI for NSTEMI. However, age and biological sex alone did have a significant effect on the rates of post-operative mortality and complications with females experiencing greater rates of post-operative adverse events. Thus, an existing diagnosis of DM does not appear to increase the post-operative risks involved in recovery from PCI for NSTEMI.

	Overall	Diabetes		p
		No	Yes	
Adverse Event, %	3.90	4.13	3.58	0.552
Died, %	1.41	1.18	2.72	0.340
Complication, %	2.71	3.25	1.99	0.106
Myocardial Infarction	1.64	2.17	0.93	0.042
Cardiogenic Shock	0.90	1.28	0.40	0.073
Heart Failure	2.71	3.25	1.99	0.106
Stroke	1.07	1.38	0.66	0.168
Cardiac Tamonade	0.28	0.30	0.26	0.999
Vascular Complications	0.40	0.49	0.26	0.701
Bleeding	1.81	2.36	1.06	0.042

Table 1: Rates of post-operative PCI for NSTEMI adverse events stratified by comorbid DM diagnosis.

PATIENT DEMOGRAPHICS AND PROGNOSTIC FACTORS OF MUCOEPIDERMOID CARCINOMA IN THE HEAD AND NECK: A NATIONAL CANCER DATABASE STUDY

Sebastian Respicio [a], Danny Ryan [a], Christopher Bine [a], Stone Zhang [a], Peter Silberstein [a], Marco DiBlasi [a]
a. Creighton University School of Medicine, Omaha, Nebraska

Background:
Mucoepidermoid Carcinoma (MEC) is a malignant neoplasm of the salivary glands that arises from secretory stem cells and involves squamous and mucinous cellular morphologies. Current National Cancer Database (NCDB) literature has only touched upon MEC's demographics within the salivary glands and oral cavity, excluding other structures in the head and neck.

Significance of Problem:
Due to its rarity, the literature on demographics and overall survival of patients with MEC arising from beyond the parotid gland are scarce and impedes clinicians from knowing what their patient has predisposing prognostic factors for MEC.

Hypothesis, Problem, or Question:
This study aims to utilize the NCDB to characterize the demographic and prognostic profile of MEC in different locations in the head and neck. Furthermore, those factors will be analyzed to correlate with the overall survival.

Experimental Design:
A retrospective study was conducted using data from the National Cancer Database (2004–2021), focusing on patients with histologically confirmed MEC. Demographic variables were evaluated through Chi-squared tests, while overall survival analysis was performed using Log-Rank tests.

Results/Data:
After filtering NCDB data for inclusion criteria, the final total patient population size was 17,713 patients. The percentage of cases of MEC for each site is Salivary Glands (64.5%), Gum & Other Mouth (22.1%), Tongue (4.6%), Nose, Nasal Cavity & Middle Ear (2.0%), Mouth Floor (1.6%), Lip (1.4%), Eye (0.6%), Thyroid (0.5%), Tonsil (0.5%), Larynx (0.4%), Nasopharynx, (0.4%), Oropharynx (0.4%), Thymus (0.3%), and Trachea & Upper Respiratory Tract, NOS (0.3%). The median age at diagnosis is 57 years old and more common in females (55.7%), white race (76.6%), and non-Hispanic ethnicity (87.4%). Furthermore, most patients had private insurance (53%), with a median household income greater than $64,000 (32.5%), and were from a metro area population greater than 1 million (55.1%). Patients traveled a mean distance of 39.023 miles and traveled within the range of 0-49 miles (74.5%). Most had a Charles-Deyo score of 0 comorbidities (81.3%), well-differentiated masses (25.8%) and most were in stage 1 upon diagnosis (42.7%). The approach to surgery was open or unspecified (55.1%), with no residual tumor after surgery (70.5%). For patients who had surgery performed, 30-day mortality after the surgery is 86.9% with a 90-day mortality of 86.1%. The majority of patients did not receive Radiation and Surgical Procedures (64.5%), Chemotherapy (89.4%), Immunotherapy (98.7%), or Palliative Care (99%). Prognostic factors that contributed to increased overall survival include female gender ($p<0.001$), other race ($p<0.001$), going to an Academic/Research program ($p<0.001$, CI 95% [156.029 - 161.331]), Private Insurance ($p<0.001$, CI 95% [192.558-196.667]), and a Median Household Income greater than $63,000 ($p<0.001$, CI 95% [171.320 - 176.885]). Furthermore, no node involvement ($p<0.001$, CI 95% [175.187 - 180.330]) resulted in a greater survival rate compared to 1 node involvement ($p<0.001$, CI 95% [131.655 - 145.551]). If the patient had surgery, Partial Organ Removal ($p<0.001$, CI 95% [181.217-188.161]) resulted in the longest survival compared to no surgery performed ($p<0.001$, CI 95% [54.951-65.362]).

Conclusions:
Key demographic and prognostic factors significantly influence the outcomes in mucoepidermoid carcinoma that contribute to management strategies and further research to address disparities and optimize patient care.

PROGNOSTIC FACTORS AND SURVIVAL OUTCOMES OF ACRAL LENTIGINOUS MELANOMA FOLLOWING SURGICAL TREATMENT: A NATIONAL CANCER DATABASE STUDY

Bryce Rigden, Reagan Blohowiak, Nicole Welch, Peter Silberstein, Marco DiBlasi (Creighton University School of Medicine, Omaha, NE)

Background: Cutaneous malignant melanoma is the most lethal form of skin cancer and consists of four subtypes: Superficial Spreading Melanoma, Nodular Melanoma, Lentigo Maligna Melanoma, and Acral Lentiginous Melanoma (ALM). Compared to other subtypes, ALM arises on peripheral surfaces of the body such as the palms of the hands and has a two to five times higher recurrence rate.

Significance: Wide-margin local excision (WLE) is the primary treatment modality for ALM; however, five-year survival rates following this surgery range from 25% to 63%. It remains unclear whether alternative surgical modalities offer potential advantages in improving survival for ALM patients based on different clinical or sociodemographic factors. These alternative surgeries include biopsy followed by gross excision, Mohs surgery, and major amputation. The purpose of this study is to investigate the epidemiological patterns and survival outcomes associated with these different surgical treatments in comparison to WLE for ALM.

Hypothesis: It is hypothesized that alternative surgical modalities may improve ALM prognosis compared to WLE alone for certain patient populations.

Experimental Design: A retrospective cohort analysis utilizing the National Cancer Database (NCDB) from 2004 to 2021 included patients diagnosed with histologically confirmed ALM that underwent surgical treatment (n=9,609). Kaplan-Meier survival curves were plotted to estimate the overall survival based on different factors, and log-rank tests were used to compare differences in the curves. Cross-tabulations were conducted to evaluate associations between surgical procedure performed and other categorical variables. Chi-square tests were used to determine the statistical significance of these associations, with statistical significance defined as $p<0.05$.

Results/Data: The number of surgically treated cases of ALM per year increased from 337 in 2004 to 741 in 2021. The majority of cases analyzed were white (84%), female (53.9%), non-Hispanic (87%), located in the South Atlantic region (20.1%), insured by Medicare (47.3%), and had a median annual household income in the top quartile (30.3%). The mean age at diagnosis was 64.57 (SD ±15.1) with an average comorbidity Charlson-Deyo Score of 0.28 (SD ±0.64). The most common primary site was the skin of the lower limb and hip (78.2%), followed by skin of the upper limb and shoulder (16.6%), and skin of the trunk (2.6%). Prognostic factors leading to better overall survival included female sex ($p<0.001$), diagnosis between 0-39 years of age (0-19 vs. 20-39: $p=0.172$, 0-19 vs. 40-59: $p=0.12$, 0-19/20-39 vs. all other age groups: $p<0.001$), white or “other” race (white vs. black: $p<0.001$, “other” vs. black: $p=0.021$), private insurance status (<0.001), median annual income in the top quartile (top quartile vs. first and second quartiles: $p<0.001$, top quartile vs. third quartile: $p=0.029$), Charlson-Deyo score of 0 ($p<0.001$), NCDB analytic stage groups of 0-I (stage 0 vs. stage I: $p=0.137$, stage 0/stage I vs. all other stages: $p<0.001$), and surgical modalities of Mohs surgery or biopsy followed by gross excision (Mohs surgery vs. WLE: $p=0.004$, Mohs surgery/biopsy followed by gross excision vs. all other surgeries: $p<0.001$). Cross-tabulations showed significant overall associations between the surgical procedure performed and NCDB analytic stage group ($p<0.001$), Charlson-Deyo comorbidity score ($p=0.005$), and facility type ($p<0.001$). In the NCDB analytic stage groups, Stage 0 patients were significantly more likely to undergo Mohs surgery, while Stage I patients had a higher proportion of both Mohs surgery and biopsy followed by gross excision. In contrast, Stage III patients were more frequently treated with WLE and major amputations. Patients with a Charlson-Deyo score of 0 were significantly more likely to have Mohs surgery or biopsy followed by gross excision. Regarding facility type, academic/research programs performed a significantly higher proportion of Mohs surgery and biopsy followed by gross excision, whereas comprehensive community cancer programs performed a significantly lower proportion of Mohs surgery.

Conclusions: This study characterizes important epidemiological patterns of surgically treated ALM. Mohs surgery and biopsy followed by excision were associated with better overall survival compared to WLE in ALM patients, but these methods are more commonly used in patients with lower-stage disease and fewer comorbidities. Mohs surgery remains a promising option for maintaining cosmetic and functional outcomes in these early-stage ALM patients. Future research should assess the benefits of this surgical approach in higher-stage and higher-risk patients to better understand its broader potential for improving outcomes while minimizing impairment to patient appearance and function.

INVESTIGATING THE ROLE OF ANDROGEN DEPRIVATION THERAPY ON AXL REGULATION IN PROSTATE CANCER

Amanda Robotham, Diane Costanzo-Garvey, Jixin Dong, Angie Rizzino, Grinu Mathew (UNMC, Omaha, NE)

Background, Significance, Hypothesis: Prostate Cancer (PC) continues to present a major health concern as the second leading cause of cancer-related death in men in the United States. It is estimated that PC will result in about 35,250 deaths in 2024. While the 5-year survival rate is around 100% for local and regional PC disease stages, metastatic PC remains lethal with few effective treatment options. Early PC is androgen-dependent, often treated with first-line androgen deprivation therapy (ADT) or castration. Even as PC progresses toward a treatment-resistant metastatic state known as castration-resistant PC (CRPC), patients continue to receive ADT through second-generation AR-targeting inhibitors such as Enzalutamide. Despite the significant therapeutic advancement, resistance to Enzalutamide is a major roadblock in the treatment of metastatic CRPC. Therefore, uncovering the biology and molecular vulnerabilities of ADT-resistant cells will help identify effective therapeutic strategies against metastatic CRPC.

Studies in multiple cancers have shown that the receptor tyrosine kinase AXL is overexpressed in drug-tolerant persister cells and can induce a dormancy-like phenotype. However, in PC, some reports point to the role of AXL as an oncogene, while others support a tumor suppressor function for the kinase. Preliminary data from our lab highlights the genetic loss of *AXL* in metastatic PC and is conserved in treatment-resistant CRPC. Similarly, the combined analysis of transcriptomic (RNA-seq) and epigenomics (ATAC and ChIP-seq) data from mCRPC samples by Tang *et al.* revealed that low expression and low accessibility of the AXL promoter locus was observed in ~70% of the samples analyzed, i.e. CRPC-AR (AR amplification/ AXL low),- Neuroendocrine and -WNT regulated (AR & AXL low) subtypes. This data corroborates our finding that AXL loss is pronounced in treatment-resistant mCRPC. Interestingly, AXL was exclusively expressed in the AP-1 and YAP/TAZ driven CRPC-Stem Cell-Like subtype; ~30% of the samples analyzed, i.e. AR low/ AXL high cells. This indicates that, although AXL loss is a significant feature of mCRPC subtypes, a fraction of cells express AXL. Understanding the molecular basis of this heterogeneity in AXL expression is critical. Importantly, how AXL-expressing PC cells respond to ADT and develop resistance remains unknown. The present study aims to investigate the role of androgen deprivation therapy and the interaction between AR, TEAD, and AP-1 transcription factors in mediating AXL expression.

Experimental Design: To test this hypothesis, a series of in vitro experiments were conducted. Since the loss of the tumor suppressors *PTEN* and *TP53* has been associated with metastatic PC, all experiments were conducted in *PTEN/TP53*^{NULL} cell lines to recapitulate the metastatic genotype. AXL-expressing cells were treated with the AR antagonist Enzalutamide or AR-degrader PROTAC ARV110 (ADT). The effect on AXL expression was assessed using immunoblotting. Additionally, cells were co-treated with ADT and YAP/TAZ/TEAD or AP-1 inhibitors to identify downstream regulators of AXL. Lastly, to simulate resistance to ADT, we generated an Enzalutamide-resistant cell line, and these cells were co-treated with ADT and YAP/TAZ/TEAD or AP-1 inhibitors.

Data and Results: In vitro studies confirmed that androgen deprivation treatment reduces AXL expression in cells that express AR and AXL. Intriguingly, there was no change in AXL expression in AR-low cells following ADT, indicating that the observed AXL loss in AR-expressing cells is not an off-target effect of ADT. This raises the question of how AR inhibition influences AXL loss. The existence of AR low /AXL high cell lines argues that AR does not directly control AXL expression. The AP-1 family of transcription factors and YAP/TAZ/TEAD have been shown to transcriptionally regulate AXL expression, suggesting them as actionable targets. Our data shows that targeting AR-low AXL-positive cells with ADT and YAP/TEAD or AP-1 inhibitors decreased the expression of AXL. In Enzalutamide-resistant cell lines we observed a reduction in AXL expression, however combining ADT with a YAP/TAZ/TEAD or AP-1 inhibitor lead to a drastic reduction in AXL expression.

Conclusion: The current results support the hypothesis that an interaction between AR, TEAD, and AP-1 transcription factors mediates AXL expression following androgen inhibition. While further studies are needed to better understand and develop potential treatment strategies for AXL-expressing CRPC, this work highlights the novel role of YAP/TAZ/TEAD and AP-1 in regulating AXL expression in the context of ADT.

RISK FACTORS FOR POSITIVE PARENTAL POSTNATAL DEPRESSION SCREENING IN THE NICU AND AT 6-9 MONTHS

Russell, Alexandra; Miller, Kerry; Solness, Cara; Hardy, Paige; Lyden, Elizabeth; Siebler, Abbey; Brei, Brianna; Peeples, Eric (Creighton University School of Medicine, Omaha, NE)

Background, Significance, and Question: Postnatal depression affects ≥10% of mothers and can significantly alter maternal-infant bonding, maternal quality of life, and infant development, behavior, and overall health. Mothers and fathers of infants admitted to the newborn intensive care unit (NICU) may experience higher levels of postnatal depression than the general population and therefore be at greater risk for these negative outcomes. However, little is known about the longitudinal post-discharge progression of postnatal depression in mothers and fathers of NICU-hospitalized infants. This study therefore aims to identify clinical associations with positive maternal or paternal Edinburgh Postnatal Depression Scale (EPDS) screening of NICU-hospitalized infants in-hospital, as well as risk factors for increased or stagnant maternal EPDS between NICU discharge and 6-9 months.

Experimental Design: Clinical and sociodemographic data and EPDS results were obtained from two local NICUs and a statewide high-risk infant follow-up clinic between 2014 and 2024. Infants without completed EPDS screenings at both initial hospitalization and the 6-9 month follow up visit were excluded. Demographics and early clinical outcomes were compared between parents with scores ≥10 versus <10. Additionally, subjects were stratified by EPDS trajectory (decreased versus unchanged/increased between discharge and the 6-9 month clinic visit) and risk factors were compared between groups. A multivariable logistic regression model was generated using significant variables from univariable analysis.

Results: In this study of 258 infants, 60/258 (23%) mothers and 4/22 (18%) fathers screened positive for depression during the NICU stay. Non-married status, prior depression history, retinopathy of prematurity, and low gestational age were independent predictors of positive maternal in-hospital EPDS screening in the regression model (Table 1). Maternal, not paternal, EPDS declined significantly from hospital to follow-up (Fig 1). EPDS scores that increased or stayed the same between hospital discharge and the 6-9 month follow up visit were associated with death of multi-birth sibling and pre-existing maternal mental health diagnosis.

Conclusions: Several indicators of infant health collected in the NICU were predictive of positive in-hospital EPDS screening but did not strongly predict changes in EPDS over time post-discharge, suggesting there are likely unmeasured post-discharge variables primarily driving post-discharge depression symptoms. Continued research on how postnatal depression develops over time will facilitate strategies for improved support for families and long-term outcomes.

Table 1: Multivariable logistic regression predicting positive maternal EPDS screening (>= 10) during the initial NICU hospitalization.

Predictor	Odds Ratio (95% CI)	p value
Marital status: Married vs. Not Married	0.44 (0.23 - 0.84)	0.012
Depression history: Yes vs. No	3.98 (1.99 - 7.97)	<0.001
Retinopathy of prematurity: Yes vs. No	4.00 (1.08 - 14.86)	0.038
Gestational age (1 week increment)	0.89 (0.83 - 0.96)	0.002

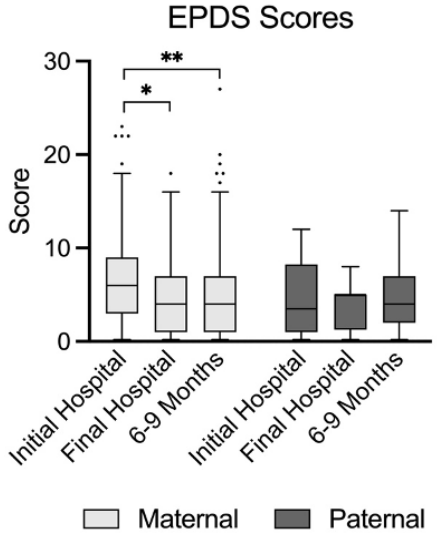

Figure 1: Comparison of median maternal and paternal EPDS scores at time of initial in-hospital screening, final in-hospital screening (if >1 in-hospital screening performed), and 6-9 month follow up visit. Line at median and whiskers demonstrate Tukey distribution. *p<0.05, **p<0.0001

SURVIVAL OUTCOMES BASED ON SURGICAL TREATMENT OF DERMATOFIBROSARCOMA PROTUBERANS: AN NCDB ANALYSIS

Julia Russolillo, Xinxin Wu, Peter Silberstein (Creighton University, Omaha, NE)

Background, Significance, Hypothesis: Dermatofibrosarcoma protuberans (DFSP) is a rare, malignancy skin cancer commonly found on the trunk. DFSP includes primary DFSP and Bednar tumors, a pigmented, intermediate-grade subtype of primary DFSP that commonly present on the extremities, appearing with a black-blueish color due to melanocytic dendritic cells, and have an increased tendency for local invasion and secondary recurrence. DFSP can be surgically resected with Mohs micrographic surgery (MMS) or wide-local excision (WLE). Despite MMS being considered the “gold standard” for treatment of malignant skin cancers, WLE is still frequently used to treat DFSP, and the difference in outcomes has not been well explored. To fill in this literature gap, data from the National Cancer Database (NCDB) was analyzed to explore overall survival based on surgical modality.

Experimental Design: A retrospective cohort study of 8,878 patients diagnosed with primary DFSP and Bednar tumors between 2004 and 2021 was conducted. The impact of surgical treatment type on survival was analyzed by Kaplan-Meier survival analysis. Other demographic factors, such as age, sex, race, and comorbidity score were considered to determine any significant trends in our cohort. Exclusion criteria included missing surgery data.

Results: 5,090 DFSP patients had survival data based on surgery type, with 805 undergoing MMS and 4,285 undergoing WLE. 53.7% of patients were female, which follows the trend of increased incidence of skin cancer among women. With respect to race, 70.3% of patients were White, 21.7% were Black, and 4.3% were Asian. The average age of our cohort was 43.2 years old (SD=15.7, range=0-90), which is younger than the average age of diagnosis of other skin cancers, such as melanoma at 66 years old. Lastly, over 90% of the patients had a Charlson-Deyo score of zero, meaning they had no comorbidities and were relatively healthy. MMS was associated with significantly increased survival compared to WLE (p=0.012), living approximately 6 months longer than those treated with WLE (210 months vs 204 months, respectively).

Conclusion: This study supports MMS as the preferred treatment of DFSP based on improved survival outcomes when compared to WLE. Although there are many clinical, financial, or personal factors that may require non-Mohs surgery, these results highlight the importance of increased access to a variety of surgical treatment options for all patients. Furthermore, it emphasizes the need for more clinical data on surgical outcomes of DFSP and Bednar tumors to better equip physicians to diagnose and treat these rare but dangerous skin cancers among a young and healthy population.

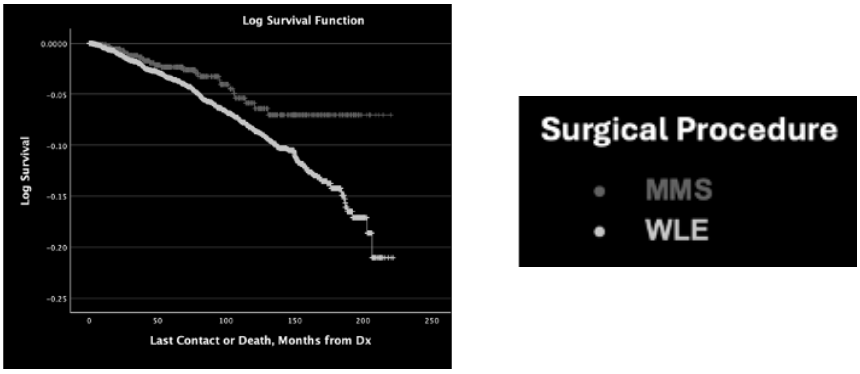

Figure 1: Survival outcomes of DFSP and Bednar tumors based on surgical procedure (gray=MMS, white=WLE).

THE EFFECTS OF MALONDIALDEHYDE AND ACETALDEHYDE ON NF-kB ACTIVITY

Kari L. Shad, Katrina J. Schneider, Daniel R. Anderson, and Dahn L. Clemens (University of Nebraska Medical Center, Omaha, NE)

Introductions: The activity of many proteins is regulated by post-translational modification (PTM) of lysine residues. One important physiologic regulatory PTM of lysine is acetylation. Acetylation of lysine is involved in the regulation of numerous proteins involved in many cellular processes, including replication, metabolism, and protein transport. Two major metabolic by-products, acetaldehyde (AA) and malondialdehyde (MDA), can combine and irreversibly bind to lysines, forming a pathologic MDA/AA PTM. Because of this, pathologic MDA/AA PTMs of lysines can compete with regulatory physiologic lysine PTMs. Therefore, we hypothesize that pathologic MDA/AA PTM competes with the regulatory physiologic PTM of acetylation and alters protein function. Alteration of normal protein function ultimately leads to cellular dysfunction. To test our hypothesis using a relevant biologic system, we investigated the effects of MDA/AA on NF-kB, a protein that is regulated by acetylation.

Methods: Immunoblots were performed to demonstrate that NF-kB is PTMed by MDA/AA. The effects of the metabolic by-products, AA and MDA, on NF-kB function was investigated using cells containing a NF-kB luciferase construct. Using a lentivirus containing a NF-kB regulated luciferase reporter gene, cell lines were generated to monitor the activation of the NF-kB signaling pathway. The cells were treated with various concentrations of MDA/AA, AA, MDA, and ADX, an acetaldehyde scavenger, at regular intervals. This was followed by stimulation with LPS to initiate NF-kB regulated transcription. To quantitatively measure the level of activity, luciferase assays were performed, and results analyzed.

Results: Immunoblot analysis confirmed MDA/AA PTM of NF-kB. The luciferase assays demonstrated attenuation of NF-kB transcriptional activity in cells treated with various concentrations of MDA/AA, AA and MDA. Importantly, inclusion of the aldehyde scavenger ADX rescued this attenuation, increasing NF-kB transcriptional activity in cells treated with ADX and MDA/AA, AA or MDA when compared with cells only treated with MDA/AA, AA or MDA.

Conclusions: We have demonstrated that NF-kB is a target for pathologic MDA/AA PTM. Additionally, treatment with AA, MDA, or a combination of MDA and AA attenuate the ability of LPS to stimulate NF-kB transcriptional activity. This attenuation is partially rescued by inclusion of the aldehyde scavenger ADX in the culture media. Because pathologic PTM by MDA/AA and the normal regulatory PTM of acetylation both occur at lysine residues, competition between pathologic MDA/AA PTM and regulatory acetylation PTM may be responsible for the attenuation of LPS induced NF-kB transcriptional activity by these reactive aldehydes. Because many proteins are regulated by PTM of lysine residues, competition between regulatory PTMs of lysines and pathogenic PTMs, such as MDA/AA, may affect many important cellular functions.

COMPREHENSIVE ANALYSIS OF MUCINS IN THERAPY RESISTANT NSCLC

Shamema Sheree, Ashu Shah, Zahraa Wajih Alsafwani, Iniyan Muthamil, Imay Lakshmanan, Surinder K Batra and Apar K Ganti

MSIA, Patient-Oriented Research, University of Nebraska Medical Center, Omaha NE,

Background and hypothesis

Lung cancer is the leading cause of cancer death in the US, accounting for about 1 in 5 of all cancer deaths. Chemoresistance results in tumor recurrence and is a frequent cause of cancer-related death. The most common KRAS mutation in non-small cell lung cancer (NSCLC), KRASG12C (13%), causes tumor initiation and progression. Despite the availability of several approved KRASG12C inhibitors {Sotorasib (AMG510) and Adagrasib (MRTX849)}, patients often develop resistance towards these drugs. Therefore, it is important to understand the mechanisms associated with chemo and KRSG12Ci-resistance in NSCLC. Multiple studies from our lab and others have demonstrated the significance of mucins in therapy resistance in many solid tumors. Mucins are large molecular weight glycoproteins, that are aberrantly overexpressed in cancer and have been shown to play a crucial role in tumorigenesis and metastasis in NSCLC. We hypothesize that mucins are upregulated in Chemotherapeutic (cisplatin) and KRASG12Ci (AMG-510/sotorasib) resistant NSCLC patients.

Experimental Design

We performed a comprehensive analysis of mucins in the publicly available datasets of tumors from KRASi (Sotorasib) resistant (GSE204753) and cisplatin nonresponsive NSCLC patients (GSE42127) using Insilico tools. We developed stable sotorasib and cisplatin resistant cell lines by exposing these cells to the individual drugs at concentrations 4-5-fold higher than IC_{50} values., We validated the development of resistance using viability assays. The mucin profiling was carried out in these cell lines using QPCR, ddPCR, western blotting, and immunofluorescence (IEF) experiments.

Results

RNAseq analysis of datasets showed an upregulation of MUC4(p=8.89E-11,log2FC=4.12991173)and MUC16(p=3.83E-10,log2FC=2.48299838) in AMG-510 resistant PDX tumor (GSE20473). We also observed a higher expression of MUC16(p=0.012,logFC=0.994) in the patient tumors (GSE42127) that did not respond to cisplatin. The pathway enrichment analysis of sotorasib resistant tumors suggested an upregulation in cell adhesion, O-linked glycosylation of mucins, endosomal pathway, antigen processing and presentation, Interferon α/β signaling, and natural killer (NK) cell-mediated cytotoxicity. Accordingly, we observe an overexpression of several genes linked with these pathways including, mucins, CECAM, galectins, CD24, and TOX3. A Spearman correlation analysis of top-upregulated genes (n=35) indicated a strong correlation between MUC16 and TOX3 (r=0.9, p=0.015). QPCR analysis showed an overexpression of MUC1, MUC4, MUC16, and TOX3 in sotorasib (SW1573) and cisplatin (H292) resistant cells. The experiments for analyzing mucins and correlated genes at protein and tumor levels are in progress.

Conclusions:

We observed overexpression of mucins MUC1, MUC4, and MUC16 in cisplatin and sotorasib resistant cell lines and patient tumors.

ELUCIDATING THE ROLE OF EHD1 IN THYROID TUMORIGENESIS

Santosh Shrestha, Bhopal C. Mohapatra, Haitao Luan, Matthew D. Storck, Robert Bennett, Vimla Band, Hamid Band, Anupam Kotwal, (UNMC Omaha, NE)

Background, Significance, Hypothesis: Work from our laboratory has established that Epidermal Growth Factor Receptor (EGFR) Pathway Substrate 15 (EPS15) Homology Domain-containing protein 1 (EHD1) plays a crucial role in ensuring high cell-surface expression of various receptor tyrosine kinases (RTKs). A pro-tumorigenic role of EHD1 overexpression has been demonstrated in Ewing sarcoma, breast cancer, and non-small cell lung cancer. A previous study found EHD1 overexpression in thyroid cancers, correlating with larger size and lymph node spread, however, whether EHD1 overexpression represents a tumor cell intrinsic modulator of thyroid cancer cell oncogenesis has not been investigated. We hypothesized that EHD1 overexpression plays a pro-oncogenic role in thyroid cancer and that its genetic downregulation in EHD1 overexpressing thyroid cancer cell lines will impair their oncogenic traits.

Experimental design: To test this hypothesis, we generated EHD1 knockout (KO) or knockdown (KD) in EHD1-overexpressing thyroid cancer cell lines (TPC-1, KTC-1, and BCPAP) using the CRISPR/Cas9 Knockout approach or stable expression of doxycycline–inducible shRNAs, respectively. Western blotting was performed to confirm the loss or downregulation of EHD1 protein expression in KO and KD cells, respectively. To assess the impact of EHD1 KO or KD on thyroid carcinogenesis, we compared control and KO/KD cell lines for cell proliferation, migration, and tumorsphere forming ability.

Data and Results: First, to establish the pro-oncogenic role of EHD1 and its specificity, we generated CRISPR-Cas9 EHD1 Knockout (KO) derivatives. EHD1-KO markedly and significantly reduced the magnitude of cell proliferation, measured using the Cell-Titer Glo assay in TPC-1, KTC-1 and BCPAP cell lines. Furthermore, EHD1-KO in these cell lines induced a significant reduction in transwell cell migration and tumorsphere forming ability. We demonstrated the Doxycycline-inducible downregulation of EHD1 in EHD1 shRNA-expressing thyroid cancer cell lines but not in control shRNA-expressing cell lines. Functional analyses using KD cell lines are ongoing.

Conclusion: Our results support the hypothesis that EHD1 overexpression plays a crucial tumor cell intrinsic pro-oncogenic role in thyroid cancer progression. The CRISPR-Cas9-mediated knockout (KO) and doxycycline-inducible shRNA knockdown (KD) in thyroid cell models provides a suitable approach to further examine the role of EHD1 in tumorigenesis and metastasis in vivo as well as to dissect the signaling pathways altered by EHD1 overexpression, including potential crosstalk with receptor tyrosine kinases. The tools generated here should also facilitate further research on the potential role of EHD1 in modulating the tumor cell cross talk with tumor immune microenvironment which is altered in thyroid cancer.

MEASURING THE CLINICAL IMPACT OF A NOVEL ID STEP-DOWN SERVICE

Makenzie Starlin, Richard Starlin, Kaeli Sampson, Trevor Van Schooneveld (UNMC, Omaha, NE)

Background, Significance, Hypothesis: Infectious disease (ID) consultation has been associated with improved clinical outcomes and antimicrobial use as well as decreased infection recurrence. A study following inpatients after ID sign-off found frequent non-adherence to ID recommendations, which was associated with a higher incidence of hospital acquired infections and increased length of stay. The ID Step-Down Service (SDS) was created to follow patients after primary ID service sign-off who continue to receive antimicrobial therapy until they complete their course, require transition back to the primary ID service, or are discharged. We sought to evaluate the clinical benefit for this service.

Experimental Design: We performed a retrospective review of 347 patients followed by the SDS between July 1, 2022, and December 31, 2023, at a tertiary care academic medical center in Omaha, Nebraska. Demographic and clinical data was entered into a REDCap database. The primary outcome was unplanned antimicrobial regimen change and who the change was directed by. Descriptive statistics were reported as medians, and associations in categorical variables were assessed using Chi Square tests, Fischer's exact tests, independent sample t-tests, and Wilcoxon rank sum tests.

Data and Results: Of the 347 total patients followed by the SDS, 34.6% (120/347) had an unplanned antimicrobial change. The ID SDS directed the unplanned change 69.2% (83/120) of the time while the other 37 changes were not ID directed. ID-directed changes were driven primarily by development of a new ID problem (30, 36.1%), other reasons (25, 30.1%), adverse drug reactions (13, 15.7%), or treatment failure (12, 14.5%). Non-ID-directed changes were predominantly due to withdrawal of care (16, 43.2%) or development of a new ID problem (14, 37.8%). Unplanned medication changes were associated with increased length of stay, a greater number of deceased patients at discharge ($p<.001$), and lower prevalence of immunosuppression or renal failure. The primary ID service was re-consulted for only 15.0% (52/347) of patients, and this was also associated with a significantly increased length of hospital stay with a median of 48 days compared to a median of 22 days ($p<.001$) for patients that did not return to the ID service.

Conclusion: We demonstrate the number of antimicrobial changes required in patients remaining in the hospital on intravenous antibiotics which would have fallen to the primary service if the ID SDS was not available. Our results support the role of the SDS to clinically follow patients receiving antimicrobial therapy after sign-off by the primary ID service. Further study to assess the impact on patient and antimicrobial use outcomes is warranted.

Demographics (N = 347)	
Median Age (in years)	61.0
Male, n (%)	239 (68.9%)
Primary Service at Time of ID Consult	
Internal Medicine, n (%)	160 (46.1%)
Family Practice, n (%)	24 (6.9%)
Surgery, n (%)	86 (24.8%)
Critical Care, n (%)	73 (21.0%)
Other, n (%)	4 (1.2%)
Renal Failure or Immunocompromised, n (%)	127 (36.6%)
Penicillin Allergy, n (%)	45 (13.0%)
Median Length of Stay (in days)	25

Table 1. Patient demographics.

Medication Change	Yes (N = 120)	No (N = 227)	P-value
Median Age (in years)	59.0	62.0	0.46
Male, n (%)	81 (67.5%)	158 (69.6%)	0.69
Primary Service at Time of ID Consult			
Internal Medicine, n (%)	53 (44.2%)	107 (47.1%)	
Family Practice, n (%)	7 (5.8%)	17 (7.5%)	
Surgery, n (%)	30 (25.0%)	56 (24.7%)	
Critical Care, n (%)	29 (24.2%)	44 (19.4%)	
Other, n (%)	1 (0.8%)	3 (1.3%)	
Renal Failure or Immunocompromised, n (%)	35 (29.2)	92 (40.5%)	0.04
Penicillin Allergy, n (%)	17 (14.2%)	28 (12.3%)	0.63
Median Length of Stay (in days)	30	23	0.01

Table 2. Antimicrobial Regimen Changes.

EFFECT OF SEVERE ANEMIA ON NEONATAL MURINE HEMATOPOIESIS, MEGAKARYOPOIESIS AND REACTIVE PLATELET PRODUCTION

Arjun Subrramanya, Juanitaa George Raj, Balamurugan Ramatchandirin, Marie Amalie Balamurugan, Zainab D Lawal, Megan Ferris, and Krishnan MohanKumar (UNMC Omaha, NE)

Background: Severe anemia is common among preterm infants and frequently leads to heightened gut permeability due to loss of E-cadherin, which permits endotoxins (lipopolysaccharides / LPS) to enter the bloodstream which leads to sensitization of immune cells and causes systemic inflammation. Nevertheless, the comprehensive effects of anemia-associated endotoxin on hematopoiesis, particularly its influence on megakaryocyte inflammation and the production of reactive platelets, have not been thoroughly investigated.

Significance of the problem: RBC transfusions are frequently utilized to address severe neonatal anemia; however, they are associated with complications such as necrotizing enterocolitis (NEC), often resulting from platelet reactivity and dysfunction. Gaining insight into the impact of anemia-related inflammation on hematopoiesis and platelet function may aid in reducing these transfusion-related risks, ultimately enhancing management approaches and outcomes for neonates suffering from anemia.

Hypothesis: Severe anemia resulting in endotoxin release causes impaired liver hematopoiesis, inflammation of megakaryocytes, and the production of reactive platelets.

Methods: C57BL/6 mouse pups were randomly divided into two groups (n=3 per group): naïve controls and severely anemic pups, with anemia induced by facial vein phlebotomy on postnatal days (P)2, 4, 6, 8, and 10 to maintain a hematocrit <20%. On P11, liver, bone marrow, and spleen tissues were collected for single-cell suspensions, and flow cytometry was performed using hematopoietic and progenitor cell markers. Inflammatory markers in megakaryocytes were analyzed to assess LPS receptor and cytokine expression. Platelet indices (platelet-large cell ratio / P-LCR, mean platelet volume / MPV) were monitored from P2 to P10, and in a separate cohort, a let-7e-5p (mature form of the let-7 family of microRNAs (miRNAs), which causes E-cadherin loss in anemic neonatal intestine) inhibitor was administered on P6 to reduce intestinal permeability and LPS translocation, evaluating its impact on platelet indices.

Results: Severe anemia resulted in an increased gut permeability and the translocation of lipopolysaccharides (LPS), which significantly altered hematopoiesis in the liver than other hematopoietic organs such as bone marrow and spleen. A notable decrease in lineage-negative cells in anemic pups, accompanied by an increase in megakaryocyte-erythroid progenitors (** p-value<0.002) and a reduction in granulocyte-monocyte progenitors (** p-value<0.002) and common myeloid progenitors (*p-value<0.033). The LSK population exhibited an increase in multipotent progenitors (MPP) while long-term hematopoietic stem cells (LT-HSC) decreased. Megakaryocytes showed enhanced expression of LPS receptors (TLR2 (*** p-value< 0.001) and TLR9(** p-value<0.002)), pro-inflammatory cytokines (IL-6(** p-value<0.002), IL-1β(*** p-value< 0.001), TNF-∝(** p-value<0.002), IL-12a(** p-value<0.002), and IFN-ɣ(*** p-value< 0.001)), and increased ploidy, which stimulated the production of reactive platelets. By day 8, platelet indices had significantly risen and when treated with let-7e-5p inhibitor the platelet indices returned to normal levels.

Conclusion: Severe anemia leads to higher endotoxin levels in the blood, presumably in hematopoietic organs, and alters hematopoiesis with inflamed megakaryocytes, resulting in the production of reactive platelets.

COMPARISON OF CLINICOPATHOLOGIC FEATURES AND DISEASE-SPECIFIC SURVIVAL IN VULVAR MELANOAM VERSUS PRIMARY CUTANEOUS SITES: A RETROSPECTIVE COHORT ANALYSIS

Mitchell A. Taylor, Sierra Thomas, Bianca Ituarte, Divya Sharma, Peter Silberstein

School of Medicine, Creighton University, Omaha, NE
Department of Dermatology, University of Nebraska Medical Center, Omaha, NE

Background and Significance: Vulvar melanoma represents a rare and distinct subset of melanoma with unique clinical and prognostic challenges. Due to its rarity, there is a limited body of research directly comparing the clinicopathologic features and disease-specific survival (DSS) of vulvar melanoma to those of primary cutaneous melanoma. This study aims to address this gap by analyzing and comparing these features and outcomes using data from the Surveillance, Epidemiology, and End Results (SEER) database.

Experimental Design: In this retrospective cohort analysis, the SEER database was utilized to identify female patients diagnosed with biopsy-confirmed invasive vulvar melanoma (ICD-O-3 histology codes 8720/3–8780/3; primary site codes C51.0–51.9) between 2000 and 2021. For comparison, cases of melanoma originating from cutaneous sites (C44.0–44.9) were also included. Statistical analyses were performed using SPSS v29.0, employing methods such as Chi-square tests, Kruskal-Wallis tests, Kaplan-Meier and log-rank, and stepwise Cox regression models ($p<0.05$).

Data and Results: A total of 1,310 vulvar melanoma patients were identified, of which greatest number were White (81.7%), aged 80 and older (26.0%), exhibited localized disease (63.8%), were diagnosed with the nodular melanoma subtype (20.8%), and demonstrated a median Breslow thickness of 2.0 mm (IQR 1.0-4.4). Compared to primary cutaneous sites, vulvar melanoma patients more commonly presented with regional (28.1%) and distant-stage disease (8.2%; $p<0.001$), the nodular melanoma subtype (20.8%; $p<0.001$), tumor ulceration (59.3%; $p<0.001$), and increased median Breslow thicknesses (2.0mm; $p<0.001$). On univariable Kaplan-Meier analysis, vulvar melanoma patients exhibited significantly lower 5- and 10-year DSS rates (46.0% and 32.0%, respectively) compared to cutaneous melanomas of the head and neck (87.0% and 80.0%), upper extremity (95.0% and 91.0%), trunk (93.0% and 89.0%), and lower extremity (92.0% and 88.0%) ($p<0.001$). Multivariable Cox regression using backwards elimination to adjust for age, race and ethnicity, annual income, rural-urban living, disease stage, tumor location, Breslow thickness, and chemotherapy revealed that all primary cutaneous sites including head and neck (aHR 0.48; 95% CI 0.41-0.57; $p<0.001$), upper extremity (aHR 0.30; 95% CI 0.25-0.36; $p<0.001$), trunk (aHR 0.49; 95% CI 0.41-0.58; $p<0.001$), and lower extremity (aHR 0.39; 95% CI 0.33-0.46; $p<0.001$) exhibited a significantly reduced disease-specific mortality risk compared to vulvar melanoma.

Conclusion: In this large, nationally representative study utilizing the SEER database, we observed vulvar melanoma patients exhibited significantly reduced 5- and 10-year DSS rates (46.0% and 32.0%, respectively) compared to all cutaneous sites, a finding validated on multivariable analysis adjusting for important covariates. Experts hypothesize that the poor outcomes observed in vulvar melanoma may be linked to a unique set of genetic mutations as well as delays in diagnosis leading to advanced stages at presentation. Further research is needed to explore targeted interventions for this rare and aggressive melanoma subtype.

Title: URBAN VERSUS RURAL DISTRIBUTION OF CHOLANGIOCARCINOMA AND FIBROLAMELLAR CARCINOMA

Authors: Elijah Torbenson, Nigel Lang, Kevin Choi, Peter Silberstein, John Paul Braun (Creighton Omaha, NE)

Purpose: This study aims to evaluate the urban versus rural prevalence of several liver cancers.

Background, Significance of Problem, and Question:
Hepatocellular carcinoma (HCC) is the most common liver cancer and is the fifth most common overall cancer in men. HCC is primarily driven by chronic HBV and HCV infection, chronic alcohol use, and primarily affects older individuals. In contrast, some of the rarer types of liver cancers, such as the fusion driven fibrolamellar carcinoma (FLC), primarily affect younger individuals. While there has been substantial epidemiological research done on some of the rarer cancers such as FLC, not as much research has been done on the urban versus rural distribution of FLC. The same can be said for cholangiocarcinoma (CCA). The goal of this study will be to compare the urban vs rural geographical distribution of various rare liver cancers (FLC and CCA) to the more prevalent liver cancers, such as HCC.

Experimental Design: Patients diagnosed with cholangiocarcinoma, fibrolamellar carcinoma, and hepatocellular carcinoma were selected from the National Cancer Database (NCDB) using the histology codes 8160, 8171, and 8170. Chi-Square goodness of fit tests were performed, as well as Kaplan-Meier analysis. Data was analyzed using SPSS version 29 and statistical significance was set at $\alpha = 0.05$.

Results/Data:
In this study, 9075 patients were diagnosed with cholangiocarcinoma, of which 174 were from rural areas and 8901 from urban areas. Based on Rural-Urban continuum codes 8 and 9 from the United States Department of Agriculture, 1.5% of the US population reside in rural areas, and this percentage was used as the standard of comparison in the Chi-Square goodness of fit test. Cholangiocarcinoma was found to be significantly enriched in rural areas ($p < 0.001$). Interestingly, Kaplan-Meier also showed that patients with cholangiocarcinoma in rural areas had higher median survival times (22.6 months, 95% CI: 21.64–23.56) than those from urban areas (14.36 months, 95% CI: 14.22–14.50), with a significant Log-Rank test ($\chi2=676.692$, $p<0.001$). Fibrolamellar carcinoma (934 patients) and hepatocellular carcinoma (270, 135 patients) were not found to have significant urban or rural enrichment in comparison to the expected proportion of urban vs rural inhabitants in the United States.

Conclusions: This study showed that cholangiocarcinoma prevalence is enriched in rural areas, and that patients from rural areas with cholangiocarcinoma have longer median survival times than those in urban areas, suggesting that there could be potential differences in environmental and socioeconomic factors that lead to this disparity.

PRENATAL OPIOID EXPOSURE SIGNIFICANTLY IMPACTS PLACENTAL PROTEIN KINASE C AND DRUG TRANSPORTERS, LEADING TO NEONATAL OPIOID WITHDRAWAL SYNDROME SUSCEPTIBILITY

Lavanya Uppala*, Sangeetha Vishweswaraiah'
*Creighton University, School of Medicine, Omaha, NE, 'William Beaumont University Hospital Research Institute Royal Oak, MI

BACKGROUND

Neonatal opioid withdrawal syndrome (NOWS) is the constellation of symptoms which results from *in utero* exposure to prenatal maternal opioid use, often resulting in lifelong physical and psychiatric consequences for the fetus, including feeding difficulties, tremors, withdrawal symptoms, and learning disorders. Differential maternal placental pharmacokinetics, including variability in genetic and epigenetics for opioid receptors, metabolic enzymes, regulatory proteins, and transporters are thought to influence susceptibility to this illness. Examination of the placenta, the physiologic interface between the fetus and mother, and especially the mechanism of drug transport with this organ, may provide insight into the etiology and susceptibility of NOWS.

SIGNIFICANCE OF PROBLEM

While an ongoing phenomenon, the opioid epidemic and its generational impact are only now beginning to be understood in their entirety. Substance abuse during pregnancy continues to rise, whether prescribed or illicit, resulting in a concomitant hidden epidemic of NOWS. This diagnosis leads to significant increases in healthcare costs and burden due to lifelong symptoms and social consequences.

HYPOTHESIS, PROBLEM, OR QUESTION

Increased prenatal surveillance via analysis of genetic susceptibility of NOWS may allow for the identification of at-risk patients, and thus for prophylactic treatment of these individuals. In this study, we examine placental ATP-binding cassette (ABC) drug transporters and solute carriers (SLCs). Protein kinase C (PKC) helps regulate both of these types of carriers involved in drug absorption, metabolism, and elimination. Investigation into epigenetic modification of PKC and these drug transporter genes allows for clarification of factors involved in NOWS development.

EXPERIMENTAL DESIGN

96 pregnant women were retrospectively identified via chart review from the William Beaumont Hospital. Placental tissue samples were categorized into three groups: 32 healthy individuals (-Opioids/-NOWS, control), 32 prenatally exposed neonates not requiring treatment (+Opioids/-NOWS), and 32 prenatally exposed infants requiring treatment (+Opioids/+NOWS). These samples were assessed for differential methylation patterns of SLC transporters, ABC drug transporters, and PKC family genes.

RESULTS/DATA

Comparing demographic characteristics of the sample groups yielded no significant differences. Whole genome-wide methylation profiling identified 87 genes which show differential methylation associated with drug transporters and PKCs. Evaluation of these genes via gene ontology examination and protein-protein interaction networks revealed the presence of potential functional groupings, primarily related to enrichments in substance transport activities.

CONCLUSIONS

Genome-wide analysis of drug transport epigenetics allowed for the elucidation of factors associated with NOWS susceptibility. Dysregulation of such genes provides potential targets for the enhanced identification of at-risk mothers and babies, and for subsequent prenatal surveillance. As this illness may have lifelong consequences, prevention and early treatment is crucial to improving patient outcomes.

TREATMENT PATTERNS IN SQUAMOUS CELL CARCINOMA VS ADENOSQUAMOUS CELL CARCINOMA OF THE PROSTATE

Ena Wang, Peter T. Silberstein, and Xinxin Wu (Creighton University School of Medicine Omaha, NE)

Purpose: Squamous cell carcinoma (SCC) of the prostate and adenosquamous carcinoma (ASC) of the prostate are two rare aggressive cancers that are poorly understood and without established treatment guidelines. Previous studies have suggested that ASC and SCC develop following treatment of adenocarcinoma of the prostate. Despite arising from similar histologic origin, it is commonly thought that ASC behaves more aggressively than SCC. The National Cancer Database (NCDB) was analyzed to determine and compare treatment patterns of these rare cancers.

Methods: A retrospective cohort analysis utilizing the NCDB from (2004-2021) included patients diagnosed with histologically confirmed SCC and ASC of the prostate between ages 0-99 years (N=286). Analysis was completed to determine the demographic profile of patients and the frequency of types of treatment received. Variables were analyzed using Pearson Chi-squared tests.

Results: 204 patients with SCC and 82 patients with ASC were identified. The median age was 70.9 years (min=39, max=90, std dev=11.4). Surgical procedure of the primary site was performed in the majority of cases for both SCC and ASC (55.4% and 52.4% respectively). Radiation was used approximately 40% of the time for both SCC and ASC. Chemotherapy was not frequently used but was nearly twice as likely to be used in SCC than ASC (28.9% vs 17.1%, p=0.038). Hormone therapy was three times more likely to be used for ASC patients than SCC (54.9% vs 14.7%, p<0.001). Palliative care was provided in a few cases for both SCC and ASC (12.3% and 9.8% respectively).

Conclusions: Our study highlights no single modality emerging as standard care. We observed that surgery was utilized in more than half of the cases and nearly half of the patients underwent radiation therapy, suggesting that these are the predominant strategies in clinical practice. Further study is needed to determine the impact of treatment on overall survival and comparison of demographics between the recipients of these two cancers.

Treatment Modality	Squamous Cell Carcinoma	Adenosquamous	P value
Received Surgery	113 (55.4%)	43 (52.4%)	0.65
Received Radiation	77 (37.7%)	36 (43.9%)	0.335
Received Chemotherapy	59 (28.9%)	14 (17.1%)	0.038*
Received Hormone Therapy	30 (14.7%)	45 (54.9%)	<0.001*
Received Palliative Care	25 (12.3%)	8 (9.8%)	0.245

INFLUENCE OF MOOD DISORDERS ON OUTCOMES OF POLYCYSTIC OVARIAN SYNDROME - A NATIONAL INPATIENT SAMPLE STUDY - 1999-2020

Bob Weng, Reid Morrissey, Jenna Lehn, Charles Button, Abubakar Tauseef, Ali Bin Abdul Jabbar, Rutvij Patel (Creighton University School of Medicine Omaha, NE)

Background, Significance, Hypothesis: Polycystic ovarian syndrome (PCOS) refers to the constellation of dysfunctional metabolic processes that leads to an imbalance of sex hormones in favor of hyperandrogenism, oligomenorrhea or anovulation, and multiple cysts on the ovaries, according to the Rotterdam criteria. Beyond their reproductive impact, the metabolic derangements of PCOS have been linked to several adverse mood effects, including anxiety, depression, and bipolar disorder, which places greater economic burden and volume load on the healthcare system. Our study investigates the dynamics of various demographic factors that influence the correlation between PCOS and mood disorders.

Experimental Design: Data for females between ages 18-50 years old were abstracted between 2016-2021 from the National Inpatient Sample (NIS). Patients with a PCOS diagnosis and comorbid mood disorders per ICD-10 codes were compared to patients with mood disorders without an existing PCOS diagnosis. Multivariate analysis was performed to substratify patient characteristics based on age, insurance, hospital type, admission time, income, and specific mood disorder. Subsequently, length of stay and hospital costs were measured as endpoint parameters between the PCOS and non-PCOS groups to generate odds ratios for comparison. Statistical significance was set at $p<0.05$.

Data and Results: Hospital admissions showed a significantly lower average age among PCOS patients with mood disorders compared to non-PCOS cohort; PCOS patients also had longer hospital stays and incurred greater costs. In the racial category, white patients consisted of the overall majority in both groups with significantly more whites with comorbid mood disorders in the PCOS group than the non-PCOS group, whereas blacks, Hispanics, and other races with comorbid mood disorders demonstrated more patients without PCOS compared to the PCOS group. Insurance distribution showed increased Medicaid use among non-PCOS patients and private insurance among PCOS patients. For median income, the lowest quartile was observed to be mostly non-PCOS patients, whereas the upper 75% of the distribution was predominated by PCOS patients.

Conclusion: Patients admitted to hospitals with PCOS and a comorbid mood disorder were generally younger and presented with greater complexity that led to longer delays in discharge times and associated healthcare costs. Notably, as these patients aged, their incurred costs also increased, making total lifetime cost substantially higher. Furthermore, PCOS patients tended to be white, earned more income, and preferred to use private insurance compared to non-PCOS patients. We hope our analysis of the contextual demographics has elucidated some of the etiologies of the discrepancies in expenses and outcomes of PCOS and concurrent mood disorders, which may be used to direct policy changes in optimizing their care while minimizing their hospital burden.

AN ENVIRONMENTALLY RELEVANT MIXTURE OF PER- AND POLYFLUOROALKYL SUBSTANCES (PFAS) IMPACTS CELL PROLIFERATION AND GENE TRANSCRIPTION IN A HUMAN MYOMETRIAL CELL LINE.

Hannah B. Wood[1], Jitu W. George, Kendra L. Clark

[1]University of Nebraska Medical Center, Omaha, NE

Background, Significance, Hypothesis: Per- and polyfluoroalkyl substances (PFAS) are a group of environmentally persistent synthetic chemicals. PFAS are found in many consumer products including non-stick cookware, food packaging materials, upholstery, and personal care products. Accordingly, PFAS are a major source of water and soil contamination. In women, many adverse reproductive effects have been associated with PFAS exposure including reduced fertility, changes in the menstrual cycle, reproductive hormone disorders, and reproductive tract diseases. Epidemiological studies have linked forever chemicals with increased risk in uterine diseases including fibroids however, the mechanisms involved remain to be elucidated. We hypothesized that exposure to a mixture of PFAS would promote cell growth and alter gene expression in UT-TERT cells.

Experimental Design: This study investigated the effects of a PFAS mixture, including long-chain "legacy" PFAS [perfluorooctanoic acid (PFOA), perfluorooctanesulfonic acid (PFOS)] and short-chain "alternative" PFAS compounds [undecafluoro-2-methyl-3-oxahexanoic acid (GenX/HFPO-DA), perfluorobutanesulfonic acid (PFBS)], on the function and transcriptome of an immortalized human myometrial cell line (UT-TERT). Cells were cultured with an environmentally relevant concentration of a PFAS mixture (1 ng/mL each of PFOS/PFOS/GenX/PFBS), or vehicle control (Methanol <0.01% final concentration) for 96h. The impact of PFAS exposure on UT-TERT cell viability/proliferation was evaluated by the MTT assay, KI67 immunofluorescence, and flow cytometry. Cell migration and invasion were evaluated by the wound healing assay and Transwell invasion assay. Gap junction intercellular communication was evaluated via the scrape load assay. To identify genes altered after exposure to PFAS in myometrial cells, RNA-sequencing was performed followed by bioinformatic analysis.

Data and Results: Increased cell proliferation was observed in the PFAS mixture ($P < 0.05$). Cell cycle analysis via flow cytometry further supported the proliferative action of the PFAS mixture via increases ($P < 0.05$) in the percentage of cells in S-phase. The number of cells with KI67 positive staining was also increased ($P < 0.05$) in cells exposed to the PFAS mixture relative to vehicle controls. Treatment of cells with the PFAS mixture for 8 hours induced migration of myometrial cells and resulted in an increase ($P < 0.05$) of the percent area covered by migration relative to the vehicle control. Additionally, the number of cells that migrated through the membrane of the Transwell insert was increased ($P < 0.05$) after 6h exposure to the PFAS mixture relative to the vehicle treated controls. To identify genes altered after exposure to PFAS in myometrial cells, RNA-sequencing was performed followed by bioinformatic analysis. The significantly upregulated and downregulated genes were chosen based on a log2foldchange value of 2 and ($P < 0.05$). Relative to control treated cells, UT-TERT cells exposed to the PFAS mixture upregulated 161 genes and downregulated expression of 108 genes. Ingenuity Pathway Analysis revealed the top 5 Molecular and Cellular Functions to be Molecular Transport, Small Molecule Biochemistry, Cell Death and Survival, Carbohydrate Metabolism, and Drug Metabolism.

Conclusion: Overall, this study demonstrates functional and transcriptomic changes in myometrial cells after exposure to a PFAS mixture, improving our knowledge about the impacts of PFAS exposures and female reproductive health. These findings suggest that PFAS compounds have the potential to disrupt normal myometrial cell function with possible long-term consequences on overall reproductive health.

NUCLEAR PHOSPHOINOSITIDE SIGNALING REGULATES LSD1'S ASSOCIATION WITH EPIGENETIC COMPLEXES

Colin Wooldrik[1,2], Dr. Suyong Choi[2]
1.University of Nebraska Medical Center, Department of Genetics, Cell Biology, & Anatomy, Omaha, NE
2.University of Nebraska Medical Center, Eppley Institute for Research in Cancer & Allied Diseases, Omaha, NE

Background

Phosphoinositides are lipid messengers regulating every aspect of cellular physiology. Contrary to dogmatic belief it has been reported that a significant fraction of phosphoinositides is found in the non-membranous nuclei while their cellular functions remain largely enigmatic. Via proteomic screens, we identified a novel nuclear protein complex containing lysine specific demethylase 1 (LSD1, encoded by *KDM1A* gene) which is the first protein shown to remove methylations on histone residues was identified and validated to interact with a phosphoinositide generating kinase PIPKIα (encoded by *PIP5K1A*). Early studies revealed LSD1 as a repressive epigenetic writer, removing transcriptionally activating methylations such as on H3K4. Recent studies, by contrary, have discovered that LSD1 preferentially removes repressive methylations on histones such as on H3K9. The dual function of LSD1 (transcriptionally activating vs. repressing) is believed to be mediated by the epigenetic complexes LSD1 is associated with in the given cellular context. Overexpression of LSD1 is reported in many cancer types including breast, lung, and liver cancer. LSD1 is shown to regulate tumorigenesis such as proliferation, cancer stemness, drug resistance, tissue invasion, and metastasis, while exact molecular mechanisms of how LSD1 exerts tumor promoting functions remains to be elucidated.

Significance of Problem

Non-mutational epigenetic reprogramming is one of the emerging hallmarks of cancers. LSD1, as the first identified histone demethylase, plays a key role in chromosomal structural remodeling and tumorigenesis in several cancer types including breast cancer. Yet, our understanding of how LSD1 functions in tumorigenesis is incomplete. Our current data points out that a nuclear phosphoinositide species generated by PIPKIα serves as a cofactor facilitating LSD1 interactions with a transcriptionally activating epigenetic complex, promoting breast cancer tumorigenesis by regulating the expression of oncogenes such as *EGFR* which has a pivotal role in breast cancer. Our study provides key insight into the unprecedented roles of nuclear phosphoinositides in the regulation of LSD1-driven epigenetic gene expression in breast cancer.

Hypothesis

Considering the transcriptionally activating role of LSD1, we aim to identify novel interacting proteins of LSD1 and the underlying mechanisms of their interactions that cancers could be utilizing to activate oncogenic pathways. We hypothesize that phosphoinositides generated by nuclear phosphoinositide kinases, including PIPKIα, regulate the interactions between LSD1 and other epigenetic regulators such as ZMYND8. This phosphoinositide-driven epigenetic complex regulates aberrant oncogenic transcription programs in cancer cells.

Experimental Design

Our previous proteomic screens identified a novel interaction of PIPKIα with LSD1. The PIPKIα-LSD1 interaction was validated in triple negative breast cancer cells, MDA-MB-231 and MDA-MB-468, using co-immunoprecipitation, and *in vitro* binding assays. Agonist-stimulated changes of PIPKIα-LSD1 were monitored by co-immunoprecipitation and proximity ligation assay (PLA) imaged with confocal microscopy. In many instances, proteins that interact with phosphoinositide-metabolizing enzymes also bind to phosphoinositide species. Via sequence analyses the putative phosphoinositide binding region on LSD1 was identified. LSD1 and binding-region-deleted-LSD1 binding to all seven phosphoinositide species were measured via *in vitro* binding assays. Cellular interactions and changes by agonist stimulation of LSD1 with phosphoinositides were monitored by PLA. Cellular functions of the PIPKIα-LSD1 nexus in breast cancer tumorigenesis were monitored by measuring known LSD1 transcription targets after depleting PIPKIα and LSD1 expression using RNAi. LSD1 has low substrate specificity *in vitro* and LSD1 is targeted to cellular substrates via interactions with other epigenetic regulators. The switches of LSD1 interactions with known LSD1 binding epigenetic regulators were analyzed upon agonist stimulation and PIPKIα depletion via co-immunoprecipitation and PLA.

Results/Data

The LSD1-PIPKIα interaction was validated by co-immunoprecipitation of LSD1 with PIPKIα. Recombinant LSD1 and PIPKIα revealed the direcet interaction of PIPKIαand LSD1. The PIPKIα-LSD1 interaction and other known LSD1 interacting proteins' associations were increased upon agonist stimulation such as serum, EGF, and TNF-α in breast cancer cells. Also, *in vitro* binding assay of recombinant LSD1 to phosphoinositide conjugated beads showed that LSD1 preferentially binds to the enzymatic product of PIPKIα, $PI4,5P_2$. A polybasic motif (composed of a stretch of basic amino acids) within the intrinsically disordered region of LSD1 was identified as a binding site for these phosphoinositides. LSD1-$PI4,5P_2$ interactions were increased by serum stimulation and reduced by PIPKIα depletion, indicating that PIPKIα was responsible for $PI4,5P_2$ association with LSD1. The depletion of PIPKIα reduced LSD1 interaction with ZMYND8, leading to the attenuation of EGFR expression in breast cancer cells. The phosphoinositide binding-defective mutant LSD1 showed reduced interaction with ZMYND8, suggesting that the phosphoinositide binding controls LSD1 interaction with ZMYND8.

Conclusions

Given the data, we have identified a LSD1 containing epigenetic complex as a novel interactor of PIPKIα. LSD1 binds to $PI4,5P_2$ generated by PIPKIα in the LSD1-PIPKIα complex. The $PI4,5P_2$ binding of LSD1 controls the LSD1-ZMYND8 epigenetic complex formation to promote the expression of *EGFR* in breast cancer cells. Our study revels previously unknown roles of nuclear phosphoinositides in epigenetic gene expression in cancer.

ANALYSIS OF TOXICITY PROFILES IN PROSTATE ADENOCARCINOMA FOLLOWING HIGH DOSE RATE-BRACHYTHERAPY BOOST TREATMENT

Duncan Works[1], Joseph Carmicheal[1], , Michael Baine[1,2], Saber Amin[2]
[1]College of Medicine, University of Nebraska Medical Center, Omaha, Nebraska
[2]Department of Radiation Oncology, University of Nebraska Medical Center, Omaha, Nebraska

BACKGROUND & SIGNIFICANCE OF PROBLEM:
Prostate cancer continues to be the most common cancer among men in the United States and the second leading cause of cancer deaths. The treatment of prostate cancer has improved in recent years due to the development of novel treatment modalities. With increasing patient options, selecting the ideal treatment has become more complex and necessitates informed decision making based on patient goals, expert advice, and various clinical factors.

High-dose radiation – brachytherapy boost (HDR-BTb) is a growing treatment modality characterized by dose-escalated local radiation directly to the implicated organ. HDR-BTb has demonstrated superior clinical outcomes to external beam radiation and offers an alternative to radical prostatectomy. Because of its rapidly expanding utilization, extensive research has been done to determine unique patient characteristics that minimize side effect profiles while producing the best clinical results. We additionally sought to determine whether previously utilized metrics for patient inclusion and exclusion for BTb usage, including prostate size of >50 cc and American Urological Association symptom score of >15, accurately predict likelihood of toxicities in our patient population. We postulate novel cutoff points in both AUA symptom score and prostate size to more accurately predict the likelihood of patients developing posttreatment toxicities after an HDR-BTb to help optimize patient selection.

RESEARCH QUESTION:
Our specific aim was to determine if patient prostate size or baseline urinary symptoms should be a consideration when utilizing HDR-BTb. Additionally, we attempt to better describe the toxicity profiles associated with HDR-BTb and analyze the impact of differing patient characteristics on gastrointestinal (GI) and genitourinary (GU) toxicity.

EXPERIMENTAL DESIGN:
Based on patients treated with HDR-BTb between April 2019 and May 2023 at the University of Nebraska-Medical Center, chart review was completed that documented American Urological Association (AUA) symptom scores prior to, during, and after treatment. GU and (GI toxicities were standardized using the Common Terminology Criteria for Adverse Events (CTCAE) and stratified into acute (<6 months initiation of treatment) and chronic (>6 months). Data were then analyzed in univariable and bivariable logistic regression analyses based on patient prostate size and AUA score at presentation.

RESULTS & DATA:
Cumulative GU and GI acute toxicities were 67% and 40%, respectively. Chronic cumulative toxicities were 21% (GU) and 11% (GI). Acute GU toxicities were higher in patients with prostates >47cc (p=.03), but no difference was seen chronically. Patients with prostate volumes >32cc revealed increased chronic GI toxicities (p=.03), but not acutely. No differences in acute or chronic GI or GU toxicities was found when stratifying prostate volume by 50cc. Patients with AUA presenting scores >15 had increased acute GI toxicities (p=.03) but no difference in GU toxicities. Stratifying by AUA scores of 7 and 4 revealed no statistically significant difference in any GU or GI acute/chronic toxicities.

CONCLUSIONS:
These results call into question the hard AUA cutoff of 15 that has previously been utilized as an absolute contraindication to HDR-BT as we found no correlation of AUA and HDR-BTb to acute or chronic GU toxicity. Our findings do not support the notion that exceptionally large prostates (50cc+) are particularly prone to radiation-induced toxicity, however, there may be novel prostate volume cutoffs that designate clinical significance.

ABERRANTLY UPREGULATED P-REX1 CONFERS CHEMORESISTANCE IN COLORECTAL CANCER

Tianzhou Xing, Yan Xie, Haihong Jiang, Na Zhong, Peter W. Abel, and Yaping Tu
Department of Pharmacology and Neuroscience, Creighton University School of Medicine, Omaha, NE

Background, Significance, Hypothesis: 5-fluorouracil (5-FU) is the standard chemotherapy for advanced colorectal cancer (CRC), but resistance frequently develops, resulting in poor outcomes. Understanding the molecular mechanisms behind 5-FU resistance could improve treatment efficacy. Using a genome-wide siRNA screen, we identified PIP3-dependent Rac exchanger 1 (P-Rex1) as a key factor in 5-FU resistance in CRC. P-Rex1 is a guanine nucleotide exchange factor (GEF) that activates Rac GTPases and integrates signals from growth factor receptors. Previously, we reported that aberrant P-Rex1 expression promotes cancer metastasis by activating Rac1. This study investigates the role of P-Rex1 in 5-FU-resistant CRC (CRC-R) progression.

Experimental Design: P-Rex1 expression was assessed by immunohistochemistry (IHC) in human CRC and adjacent normal tissues (n = 142). Western blotting measured P-Rex1 levels in human CRC cell lines and fetal colon epithelial cells. Functional studies involved P-Rex1 knockdown via siRNA or overexpression via plasmid transfection. 5-FU sensitivity was evaluated using the sulforhodamine B (SRB) viability assay. Xenograft models (athymic nude mice) were used to assess tumor growth and response to 5-FU. Thymidylate synthase (TYMS) expression was quantified by Western blot, and Rac1 activity was measured using a Rac1-GTP pulldown assay. Statistical analyses were performed using Student's t-test and Kaplan-Meier analysis.

Data and Results: P-Rex1 was expressed in 84% of CRC tissues (78/93), compared to 14% of normal tissues (7/49), with higher levels in CRC-R specimens. Data from the Human Protein Atlas showed that elevated P-Rex1 expression correlated with increased risk of death in CRC patients. Western blotting revealed no P-Rex1 expression in human fetal colon epithelial cells. CRC cell lines with low or absent P-Rex1 (HCT8, SNU-C1) were sensitive to 5-FU, whereas P-Rex1-expressing cell lines (HT29, SW480, HCT116) were relatively resistant. Knockdown of P-Rex1 in HT29 cells restored 5-FU sensitivity, while overexpression in HCT8 cells reduced responsiveness, indicating that P-Rex1 contributes to 5-FU resistance. In vivo xenograft studies confirmed these results; silencing P-Rex1 enhanced tumor sensitivity to 5-FU, while P-Rex1 overexpression conferred resistance. Thymidylate synthase (TYMS) is a key 5-FU target and previous studies showed that TYMS overexpression is linked to 5-FU resistance, and a significantly shorter survival in patients. We found that silencing P-Rex1 reduced TYMS expression in HT29 cells, whereas overexpression in HCT8 cells increased TYMS levels. Additionally, silencing P-Rex1 decreased Rac1 activity in HT29 cells, while overexpression in HCT8 cells increased Rac1 activity. Notably, treatment with the Rac1-specific inhibitor NSC23766 (50 μM) reduced P-Rex1-induced TYMS upregulation and restored 5-FU sensitivity, highlighting a molecular pathway linking P-Rex1 to 5-FU resistance.

Conclusion: P-Rex1 plays a critical role in promoting 5-FU resistance in CRC through Rac1-dependent upregulation of TYMS. Importantly, inhibiting Rac1 can attenuate P-Rex1-driven 5-FU resistance. These findings position P-Rex1 as a promising therapeutic target to enhance the efficacy of 5-FU-based chemotherapy in CRC and potentially in other cancers where P-Rex1 contributes to drug resistance.